4. Model construction and calibration

4.1 Introduction

The Macaque model was configured for each of the eight study catchments; Thomson, Armstrong Creek Main, Armstrong Creek East, Cement, McMahons Creek, Starvation Creek, Tarago and Bunyip. This section describes the calibration procedure and the calibration results for each catchment. The data required to construct the configurations and to carry out the calibrations are described in the previous section.

A description of the calibration process used, including a summary of model parameters derived from calibrations is presented in Section 4.2. More detailed discussion in relation to the calibration of each catchment follows in Sections 4.5 to 4.12.

4.2 Calibration

For each catchment, Macaque was run on a daily time step and calibrated against total monthly streamflow data. The models were run for two years prior to the calibration period, to allow water stores to equilibrate to representative conditions. The calibrations were optimised iteratively by hand using monthly summary statistics and the coefficient of efficiency. The basis for this multi-objective approach was introduced by Peel *et al*., (2000). Peel *et al*. (2000) noted that model calibrations to optimise the coefficient of efficiency led to the predicted streamflow having much less variability than the observed flow. This is an undesirable result, and so monthly summary statistics are essential to ensure that the predicted streamflow has similar variability to the observed streamflow.

The objective of model calibration was to maximise the coefficient of efficiency (E) described by Nash and Sutcliffe (1970), while reducing the percentage difference in mean, standard deviation and coefficient of variation between the predicted and observed streamflow data. Differences in the mean, standard deviation and coefficient of variation, expressed as a percentage change from the observed data, were ideally kept to less than 5%. The coefficient of efficiency provides a guide to the quality of the model fit, and is described by Nash and Sutcliffe (1970) in Equation (1).

$$E = 1.0 - \frac{\sum_{i=1}^{N}(O_i - P_i)^2}{\sum_{i=1}^{N}(O_i - \bar{O})^2} \qquad (1)$$

where E is the coefficient of efficiency value, O_i and P_i are the observed and predicted values respectively at each time step, and the overbar denotes the mean for the entire time period of the observed data. The coefficient of efficiency was used to evaluate the performance between observed and model simulated means and variances. If the square of the differences between the model simulations and the observations

is as large as the variability in the observed data, then E = 0, and if it exceeds it, then E < 0 (i.e. the observed mean is a better predictor than P_i).

The coefficient of efficiency can range from negative infinity to 1.0, where higher values indicate a better model fit. Chiew *et al*. (1993) noted that simulations where E is greater than 0.6 are considered satisfactory, and greater than 0.8 are considered good. A value for E of 1.0 is considered a perfect reproduction of the observed data by the model.

The K-fold cross validation method described by Efron and Tibshirani (1993) was used to cross validate the calibrated models. The available recorded streamflow was divided into K roughly equal parts (in this case K = 3) so that each part contained the same number of months of streamflow data. The Macaque model for each catchment was then calibrated against two parts (two thirds) of the recorded streamflow a total of three times, with each calibration being based on a different combination of the three parts. The three calibration periods comprised the first and second thirds (1 & 2), the second and third thirds (2 & 3), and the first and third thirds (1 & 3).

The calibrated parameters were then validated, by estimating the streamflow of the remaining third. The three calibrations ensure that all three parts of the recorded data used for validation once. The quality of the calibration can then be verified by comparing the calibration against the cross validation estimated streamflows. For each catchment, the model was also calibrated to the entire record of streamflow for comparison with the K-fold cross validation results. Calibration parameters were selected that provided the best overall fit for the three calibration periods.

The Armstrong Creek East and Cement Creek catchments had streamflow records spanning only ten, and two and a half years respectively. These catchments were calibrated against the entire streamflow record. However, the record was too short for the Cement Creek catchment to allow any meaningful further analysis, and no further analysis other than calibration was conducted on this catchment.

The periods of available streamflow record and input variables to facilitate calibration and validation are listed in Table 4.1. Note that the Tarago recorded total streamflow has missing data between 1963 and 1996, and as such, the available period consists of two separate periods of streamflow record.

Table 4.1. Total periods available for calibration and validation

Catchment	Start date	End date	Time period (years)	Number of months
Thomson	1/1/1954	31/12/1998	45.0	536
Armstrong (Main)	1/01/1973	30/06/2005	32.0	271
Armstrong (East)	1/02/1973	31/05/1984	11.3	99
Cement	1/06/2002	28/02/2005	2.7	30
McMahons	1/08/1972	30/06/2005	32.8	297
Starvation	1/09/1972	31/10/2005	33.2	294
Tarago	1/03/1944	30/11/1963	-	-
Tarago	1/07/1996	30/09/2005	28.9 (total)	346 (total)
Bunyip	1/08/1948	31/05/1987	38.8	458

The parameters in Macaque available for calibration include those relating to the surface soil saturated hydraulic conductivity, the minimum soil saturated hydraulic conductivity, a shape parameter that relates the exponential decline in soil saturated hydraulic conductivity with depth, a depth parameter at which the minimum soil saturated hydraulic conductivity is reached, the ratio of hydraulic to surface gradient, and the precipitation scalar. The incoming precipitation is multiplied by the precipitation scalar to produce the predicted precipitation at each ESU. It allows the incoming rainfall to be increased or decreased uniformly as required.

Although six parameters are available for calibration, Peel *et al*. (2000) only used two of them to achieve the modelling objective in that study. Peel *et al*. (2000) found that the precipitation scalar had a large influence over the predicted mean daily streamflow, while the ratio of the hydraulic to the surface gradient had a large influence over the variability of the predicted daily streamflow. The other parameters were set to default values that do not contradict the range of field-measured values. Similarly, in this study, calibration was conducted by changing the precipitation scalars and the hydraulic to surface gradient model parameters. A summary of the final calibration parameters for all catchments, along with catchment size, the stream threshold used in Macaque, and the number of resulting ESUs, is given in Table 4.2.

In addition, flow duration curves were constructed for the complete observed streamflow record and for the predicted streamflow (using the final calibration parameters), to provide a further visual analysis of the model fit.

The model performance for each of the catchments is presented and discussed in the following sections. A summary of results for all the catchments follows.

Table 4.2. Catchment areas, stream threshold used, number of ESUs and resulting calibration parameters for precipitation scalar and for hydraulic gradient for the best simulation.

Catchment	Area (km^2)	Stream threshold (km^2)	Number of ESUs	Precipitation scalar	Hydraulic gradient
Thomson	476.52	5.0	1451	1.43	0.99
Armstrong (Main)	39.28	1.0	309	1.32	0.96
Armstrong (East)	14.49	1.0	124	1.225	0.984
Cement	14.25	0.1	801	1.03	0.90
McMahons	39.52	1.0	398	1.42	0.935
Starvation	31.31	1.0	308	1.415	0.89
Tarago (at Neerim)	78.88	1.0	766	1.435	0.901
Bunyip	39.44	1.0	392	1.51	0.83

4.3 Scaling LAI values used in Macaque

The relationships between LAI and age which are assigned to each vegetation type in Macaque, is based on field research in the Maroondah catchments (Watson 1999). The constraints of this study precluded field measurements of LAI in the other catchments for comparison with the representation of LAI by Macaque. However, an investigation was undertaken into differences between the Maroondah catchments (for which LAI values have been derived and used by Watson, 1999) and the other catchments in this study, by comparing a "wetness-index" of each of the catchments. A study by Ellis *et al*. (1999) found that the LAI of natural eucalypt forests was strongly correlated with P/E, where P is the average annual rainfall, and E is the average annual pan evaporation. In this was, the long term LAI of native forest may be estimated if P and E are known. In this study, the relationship between P/E was determined for each catchment, and then used, where appropriate, to scale the LAI values used in Macaque.

The long term average annual rainfall and pan evaporation were obtained from The Bureau of Meteorology's Data Drill. This provides daily data at a resolution of 5km x 5km. A weighted average was used to derive a single value of long term rainfall (P) and evaporation (E) for each catchment (Table 4.3). A wetness index was then calculated by P/E. The difference of the wetness index for each catchment relative to the Maroondah catchments was then calculated (final column in Table 4.3).

The relative differences between the wetness index of the catchments in this study and that of the Maroondah catchment were quite small, except that for the Tarago catchment. The wetness index for the Tarago catchment was 0.8 (or 80%) that for the Maroondah catchments. Accordingly, the values for LAI used in Macaque, were all scaled down to 80% for the Tarago catchment.

Table 4.3. Weighted average long term rainfall and pan evaporation, calculated wetness index, and relative wetness index of the study catchment relative to the Maroondah catchments.

Catchment	Rainfall (P)	Evaporation (E)	Wetness index (P/E)	Relative wetness index
Maroondah	1469	927	1.59	1.00
Thomson	1379	795	1.73	1.09
Armstrong (Main)	1545	866	1.78	1.12
Armstrong (East)	1417	920	1.54	0.97
Cement	1611	963	1.67	1.05
McMahons	1486	881	1.69	1.06
Starvation	1583	857	1.85	1.16
Tarago	1261	981	1.29	0.80
Bunyip	1449	932	1.55	0.97

4.4 Comparison of modelled LAI with NDVI

The LAI assigned to each vegetation type in Macaque is based on experience in the Maroondah catchments (Watson 1999). The constraints of this study precluded field measurements of LAI for comparison with the representation of LAI across the catchment by Macaque. In the absence of any field measurements of LAI, it is still possible to assess the spatial variation in LAI by comparing the spatial representation of LAI in Macaque, with the normalised difference vegetation index (NDVI). NDVI is a remotely sensed measure of vegetation density, which may be related to LAI. Given the time constraints of this study, calibration of NDVI data to LAI estimates was not possible. While NDVI data could not be used to assess the accuracy of the modelled LAI values, however, it was used to provide an indication of the spatial variability of the modelled LAI.

NDVI spatial data was provided by DSE for 23 December 1988. For each catchment, the Macaque model was run to produce a spatial map of LAI for that day. The two images were then compared visually to assess the spatial variation in NDVI with the spatial variability of modelled LAI.

4.5 Thomson

Streamflow data were obtained from Melbourne Water, and are a mass balance estimate of streamflow (at the dam wall) derived from upstream gauges and scaling processes. Three precipitation base stations were used (Aberfeldy, Walhalla Composite and Woods Point). A total of 62 rainfall stations in and around the catchment were used to derive the precipitation coefficient maps. A list of these rainfall stations is provided in Table 4.4.

Table 4.4. List of precipitation stations used for the Thomson catchment. * denotes a base station.

Station name	Easting	Northing	Elevation
Aberfeldy	443500	5827400	1050
Donnellys Ck	448300	5821500	488
Easton Portal	436200	5825300	485
Jericho	435400	5834200	555
Little Boys Creek	439300	5817600	960
Mount Gregory	423300	5828900	1195
Mount Matlock	428400	5841300	1372
Mt St Gwinear	441200	5811300	1270
Mount Victor	442600	5835800	1050
Mt Horsfall	461800	5818900	1128
Mt Useful	452600	5827400	1400
Thomson Portal	431500	5827600	540
Thomson/ Yarra Divide	426100	5821000	1025
Upper Thomson Camp	423900	5833800	1160
Whitelaws Ck	434350	5820850	1080
Beardmores	448162	5812500	655.3
Erica	444600	5796500	402
Jericho	435400	5834202	555
Lily Creek	445500	5825500	549
Matlock	430845	5838481	1207
Matlock Post Office	432320	5838493	1219.2
Mt Baw Baw	435200	5811600	1370
Mount Gregory	423594	5827321	1128
St Clair	425100	5837100	1200
Tanjil Bren	427500	5813300	838.2
Thomson Portal	430938	5827386	639
Upper Thomson Camp	423526	5834721	1158.2
Walhalla Composite*	451600	5800200	390
Woods Point*	433779	5841357	685.2
Aberfeldy*	443500	5827401	1050
Bells Track	438200	5822900	460
Binns	458200	5813300	800
Cream Can Hill East	433500	5830200	1040
Donnellys Ck	448300	5821501	488
Easton Portal	436200	5825301	485
Head Donnellys Ck	459600	5822400	1021
Jericho	435400	5834201	555
Junction Matlock/Licola	444100	5834600	1060
Lily Ck	445646	5825643	502
Little Boys Creek	439300	5817601	960
Long Ck	433800	5806600	720
Marshalls Spur	435900	5820800	1050
Matlock	430500	5837900	1150
Mount Victor	442600	5835801	1050
Mt Baw Baw	435200	5811601	1370
Mt Gregory	423300	5827901	1195

Station name	Easting	Northing	Elevation
Mt Horsfall	461800	5818901	1128
Mt St Gwinear	441200	5811301	1270
Mt Useful	452600	5827401	1400
Newlands North	431000	5821700	1140
Oriental Saddle	452000	5835500	1220
Rawson	446200	5798900	460
Sharpes	442000	5816000	960
Shaws	413000	5833100	980
St Clair South	428400	5832800	1160
Thomson Dam	446300	5810600	500
Thomson Portal	431500	5827601	540
Thomson/ Yarra Divide	426100	5821001	1025
Upper Thomson Camp	423900	5833801	1160
Victor Spur	439200	5834300	880
Webber Spur	436500	5774300	900
Whitelaws Ck	434350	5820851	1080

Values of model performance for each of the three calibration periods (i.e. three different combinations of two thirds of the period of record) and corresponding validation period (remaining third) for the Thomson catchment are listed in Table 4.5. These values of model performance for each calibration and validation period are for the single model run considered to exhibit the best model performance for each calibration period. The set of model parameters that give the best overall model performance, based on assessment of the four calibration periods, are given in Table 4.2. The overall performance was good, with E values above 0.75, and generally approaching 0.80. Model performance is generally slightly lower (but still good) for the non-calibration periods. Figure 4.1 shows the observed and predicted total flow for the entire record, and Figure 4.2 shows the flow duration curves for observed and predicted flows. The flow duration curves suggest the model appeared to generally under predict the low flow months, while the time series of flow indicates that the peak flows in several months tended to be either over or under predicted. Figure 4.3 shows a map of the resulting predicted precipitation across the catchment from Macaque using the best calibration parameters.

Table 4.5. Results for calibration and validation for the Thomson catchment. The numbers in the column headings refer to the first (1) second (2) or third (3) third of the whole period of record. For example, Calibration 2&3 refers to the calibration parameters for the second and third third, Validation 1 is the corresponding first third used for validation in this case.

Parameter	Calibration 1 & 2	Validation 3	Calibration 2 & 3	Validation 1	Calibration 1 & 3	Validation 2	Calibration ALL
E	0.799	0.763	0.750	0.847	0.810	0.736	0.788
% Mean	0.64	-12.1	-5.27	-0.48	-6.19	1.85	-3.61
% SD	6.16	-11.5	-0.46	3.66	-2.32	9.48	1.30
% Cv	5.48	0.73	5.08	4.16	4.13	7.50	5.10
PScalar	1.43		1.43		1.43		1.43
Hyd Grad	0.99		0.99		0.99		0.99

E = coefficient of efficiency; % Mean = percentage difference between the observed and predicted daily streamflow means; % SD = percentage difference between the observed and predicted daily streamflow standard deviations; %Cv = percentage difference between the observed and predicted daily streamflow coefficients of variation, PScalar = precipitation scalar; Hyd Grad = hydraulic gradient.

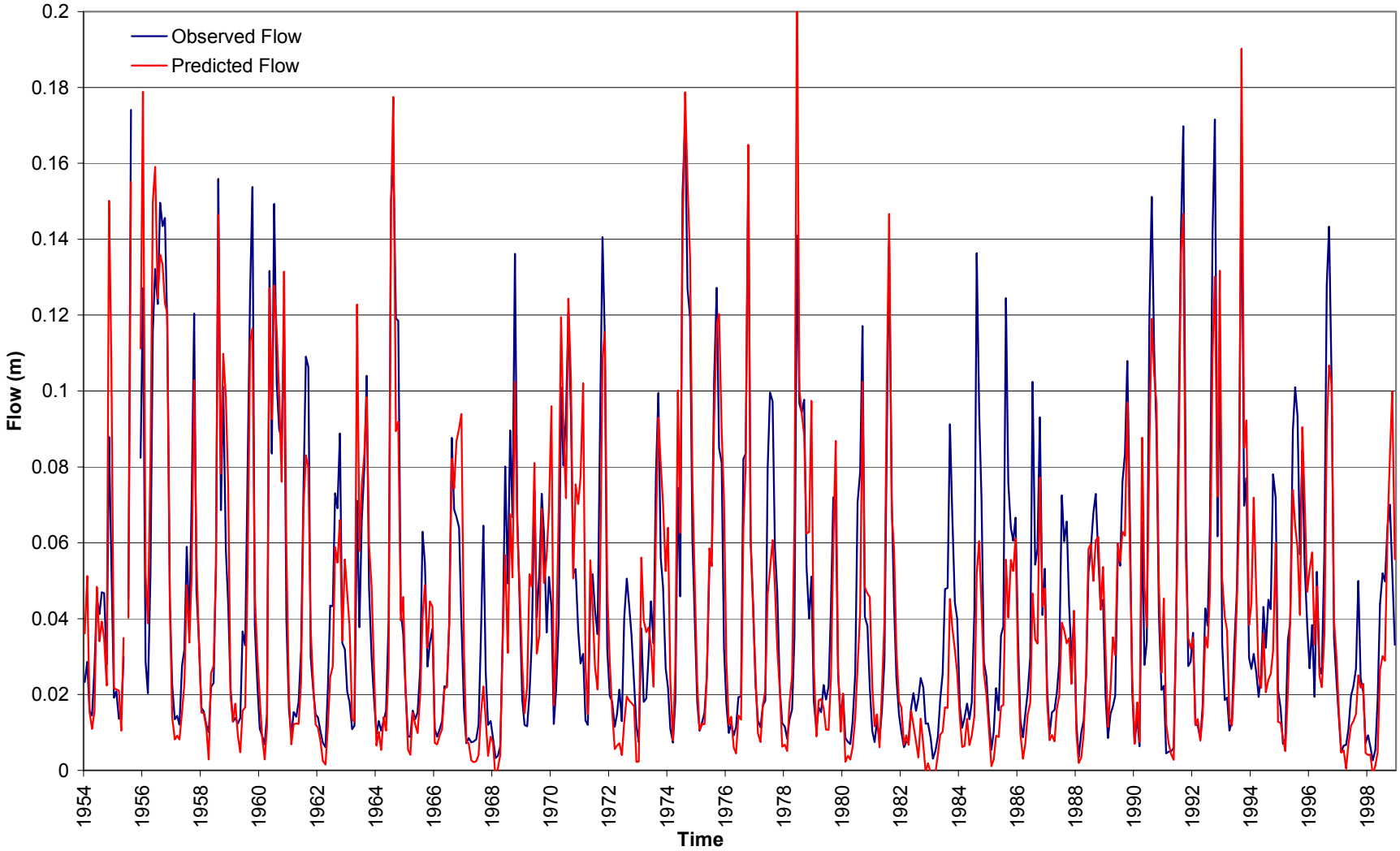

Figure 4.1. Predicted and observed total monthly flow in metres (m) for the Thomson catchment.

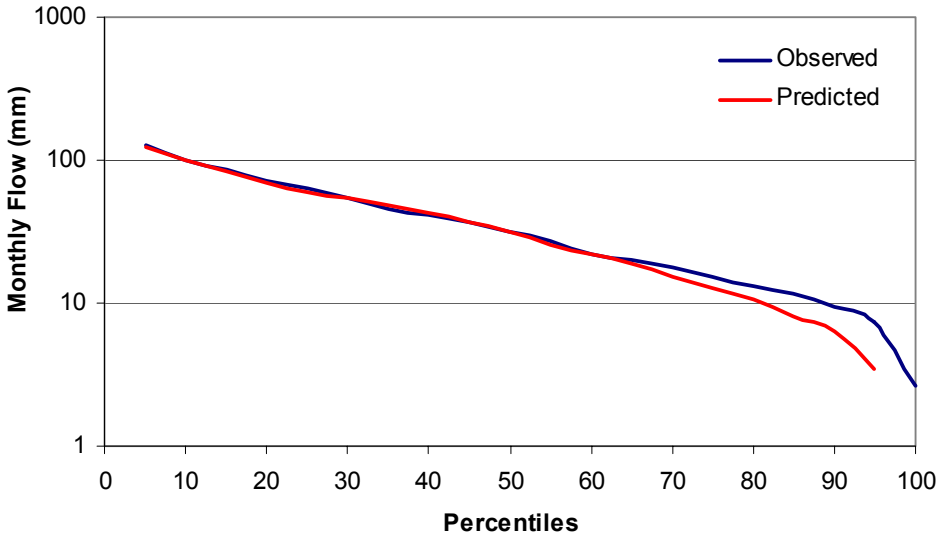

Figure 4.2. Flow duration curves for observed and predicted streamflow for the Thomson catchment.

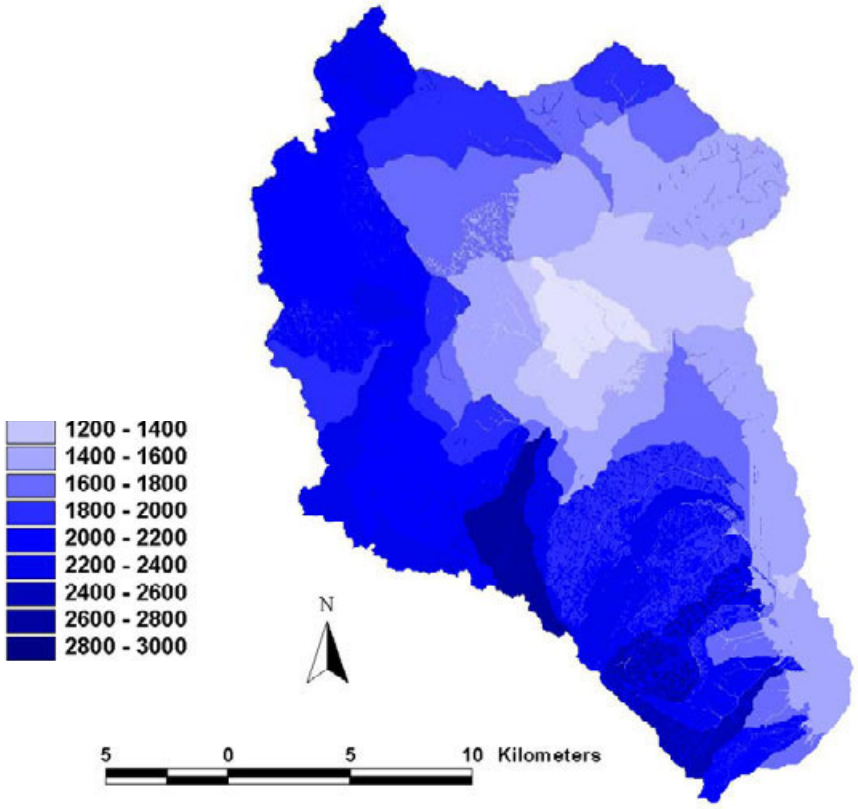

Figure 4.3. Map of mean annual precipitation (mm) (synthetic) for the Thomson catchment for the calibration period between 1954 and 1988 (45 years) produced using the MLR precipitation mapping method described in Section 3.4.3 and model calibration.

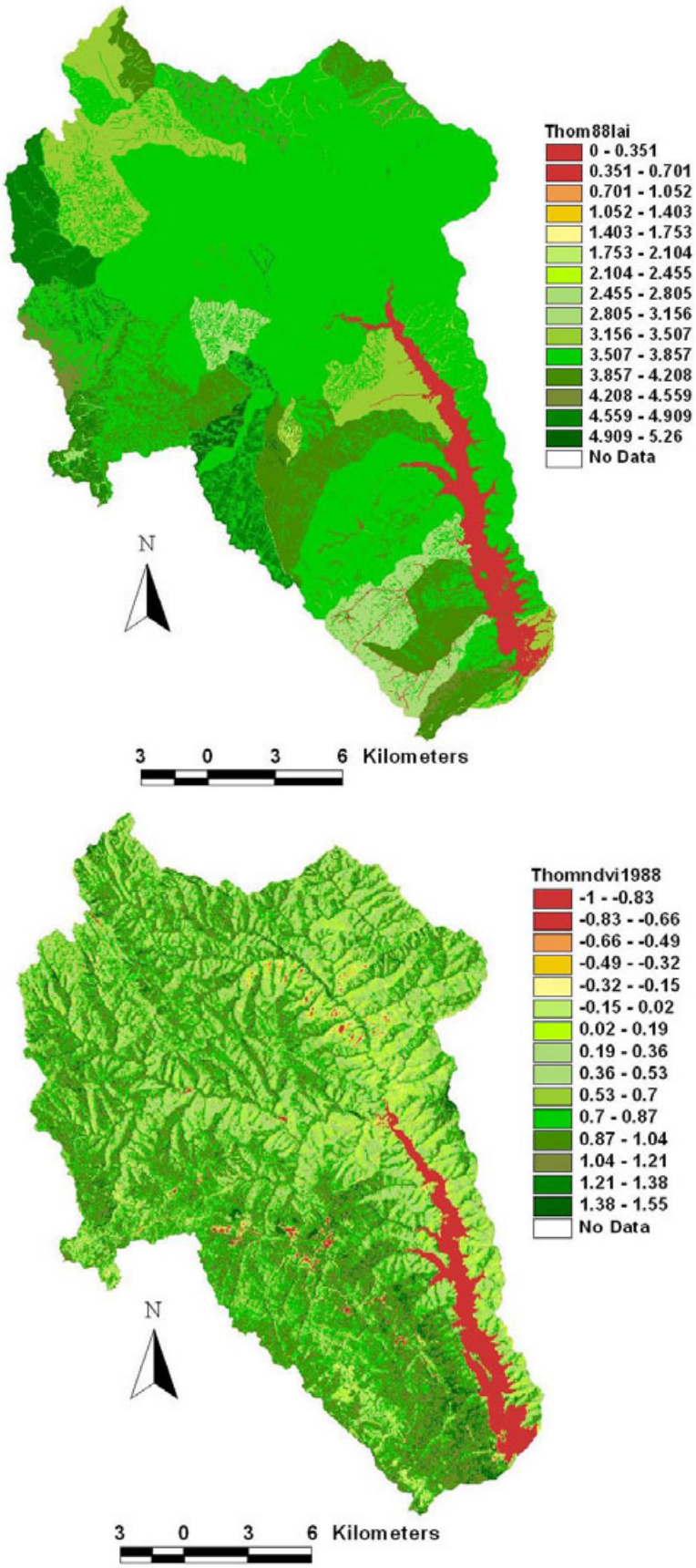

Figure 4.4. Spatial maps of a) NDVI and b) LAI for the Thomson catchment.

Figure 4.4 shows a comparison between spatial maps of a) NDVI and for b) Macaque derived LAI on 23 December 1988. There are general similarities between the two, with areas of higher vegetation density and higher LAI occurring along the south-western boundary of the catchment. This area corresponds to the area of higher rainfall and where *E. regnans* and *E. delegatensis* (species with higher natural LAI) occur.

4.6 Armstrong Creek Main

Two precipitation base stations were used (Marysville PO and OShannassy Reservoir) for the Armstrong Creek Main catchment. A total of 17 rainfall stations in and around the catchment were used to derive the precipitation coefficient maps. A list of these rainfall stations is provided in
Table 4.6.

Table 4.6. List of precipitation stations used for the Armstrong Creek Main and East catchments. *denotes a base station.

Station name	Easting	Northing	Elevation
Big R (Messmate Ridge)	407183	5847321	640
Marysville PO*	389277	5847812	420
OShannassy Reservoir*	392930	5825788	240
Poley Range	391180	5834155	1250
Reefton	404459	5830612	616
Starvation Ck BOM	395709	5824958	283
Walsh's Creek Station	403029	5826900	612
Warburton 86121	383345	5820908	170
Cumberland Junction (Cambarville)	401616	5842685	930
Junction of Roads 7 & 21	413515	5825785	823
Lake Mountain	400614	5848188	1260
Mt Strickland	388412	5841786	1036
Paradise Plains	394715	5841480	895
Shaws	413110	5833282	980
Starvation Creek MW	398368	5820908	370
Storm Creek	394612	5855882	1260
Upper Yarra Dam	402509	5829879	335.3

Values of model performance for each of the three calibration periods (two thirds) and corresponding validation period (remaining third) for the Armstrong Creek Main catchment are listed in
Table 4.7. These values of model performance for each calibration and validation period are for the single model run considered to exhibit the best model performance for each calibration period. The set of model parameters that give the best overall, model performance, based on assessment of the four calibration periods, are given in Table 4.2. The overall performance was satisfactory, with E values above 0.60. The extremely wet winter of 1975 relative to the rest of the streamflow record made a good calibration and

validation of the model difficult to achieve. Model performance is generally slightly lower for the non-calibration periods. Figure 4.5 shows the observed and predicted total flow for the entire record, and Figure 4.6 shows the flow duration curves for observed and predicted flows.

Figure 4.7 is a map of the resulting predicted precipitation across the catchment from Macaque using the best calibration parameters.

Table 4.7. Results for calibration and validation for the Armstrong Creek Main catchment.

Parameter	Calibration 1 & 2	Validation 3	Calibration 2 & 3	Validation 1	Calibration 1 & 3	Validation 2	Calibration ALL
E	0.622	0.780	0.623	0.646	0.667	0.288	0.638
% Mean	1.34%	-18.58%	-1.27%	-8.00%	-3.94%	19.84%	-3.85%
% SD	-24.83%	-6.89%	7.98%	-39.54%	-15.09%	33.60%	-21.10%
% Cv	-25.82%	14.36%	9.37%	-34.28%	-11.61%	11.48%	-17.94%
PScalar	1.32		1.32		1.35		1.32
Hyd Grad	0.96		0.96		0.975		0.96

E = coefficient of efficiency; % Mean = percentage difference between the observed and predicted daily streamflow means; % SD = percentage difference between the observed and predicted daily streamflow standard deviations; %Cv = percentage difference between the observed and predicted daily streamflow coefficients of variation, PScalar = precipitation scalar; Hyd Grad = hydraulic gradient.

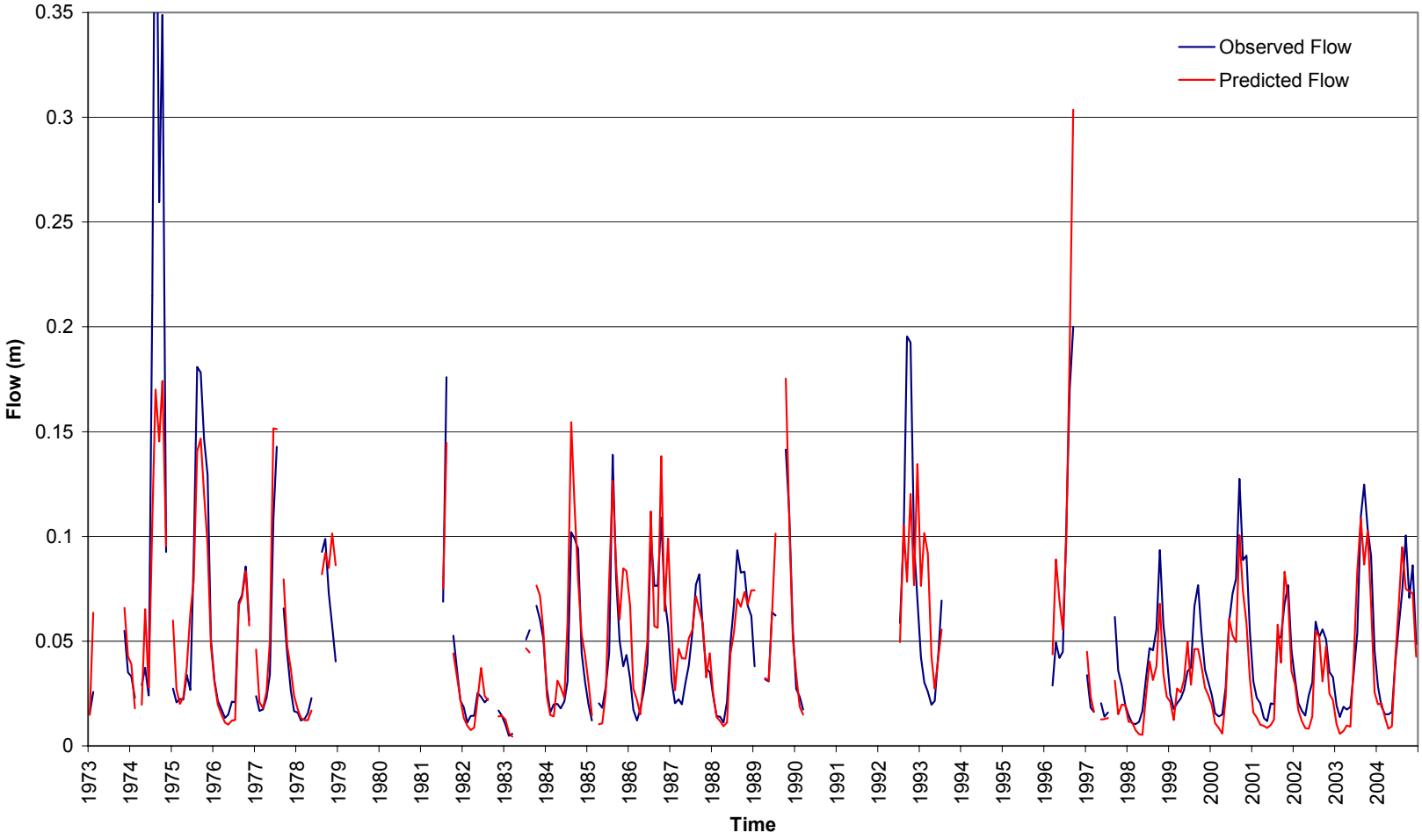

Figure 4.5. Predicted and observed total monthly flow in metres (m) for the Armstrong Creek Main catchment.

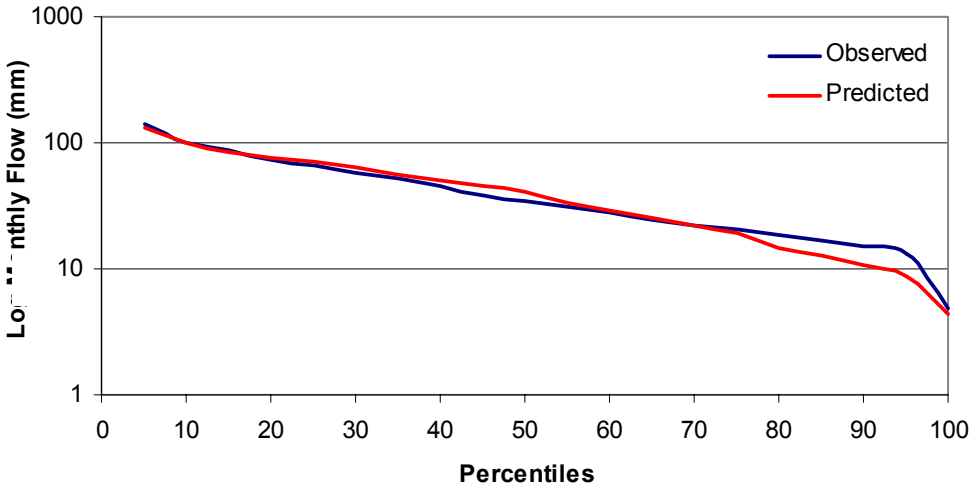

Figure 4.6. Flow duration curves for observed and predicted streamflow for the Armstrong Creek Main catchment.

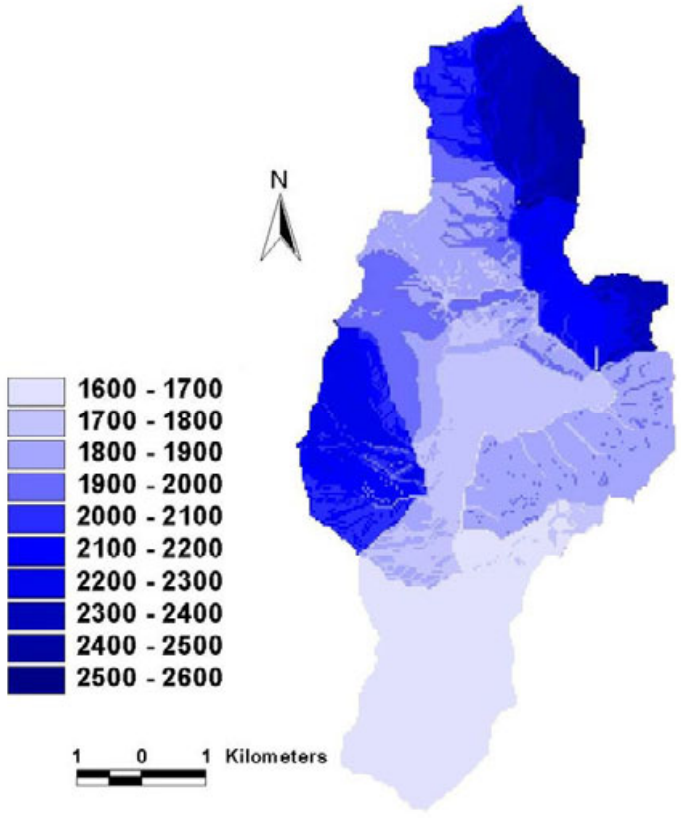

Figure 4.7. Map of mean annual precipitation (mm) (synthetic) for the Armstrong Creek Main catchment for the calibration period between 1973 and 2004 (32 years) produced using the MLR precipitation mapping method described in Section 3.4.3 and model calibration.

Figure 4.8 shows a comparison between spatial maps of a) NDVI and b) Macaque derived LAI on 23 December 1988. There are general similarities between the two, with areas of higher vegetation density and higher LAI occurring along the south-western boundary of the catchment. Also visible is the relatively low vegetation index and LAI area in the northern portion of the catchment.

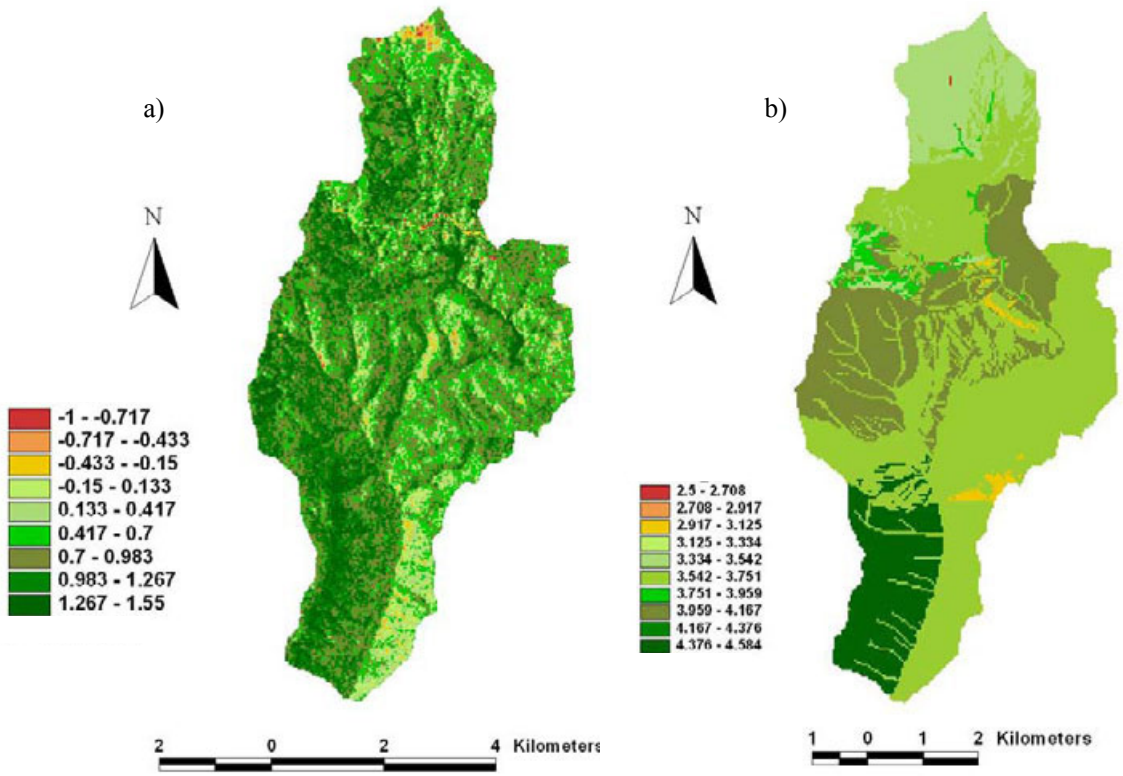

Figure 4.8. Spatial maps of a) NDVI and b) LAI for the Armstrong Creek Main catchment as at 23 December 1988.

4.7 Armstrong Creek East

Two precipitation base stations were used (Marysville PO and OShannassy Reservoir) for the Armstrong Creek East catchment. A total of 17 rainfall stations around the catchment were used to derive the precipitation coefficient maps. These were the same as those used of the Armstrong Creek Main catchment. A list of these rainfall stations is provided in
Table 4.6.

There was insufficient length of streamflow record (10 years) to conduct a proper calibration and validation process for the Armstrong Creek East catchment. Therefore, the model was simply calibrated to the entire record of observed streamflow. Values of model performance for this calibration are listed in

Table 4.2. These values are for the single model run considered to exhibit the best model performance. The corresponding model parameters are given in Table 4.8. The overall performance led to a good value for E (0.795) but only satisfactory in terms of differences in variation between predicted and observed streamflow. Figure 4.10 shows a poor fit of the model in terms of flow duration curves for observed and predicted flows. Poor model performance in these areas is due to the relatively short period of streamflow record available for calibration. It is expected that model performance would improve as more streamflow data becomes available.

Figure 4.11 shows a map of the resulting predicted precipitation across the catchment from Macaque using the best calibration parameters.

Table 4.8. Results for calibration and validation for the Armstrong Creek East catchment.

Parameter	Calibration ALL
E	0.795
% Mean	0.01%
% SD	1.54%
% Cv	1.52%
PScalar	1.225
Hyd Grad	0.984

E = coefficient of efficiency; % Mean = percentage difference between the observed and predicted daily streamflow means; % SD = percentage difference between the observed and predicted daily streamflow standard deviations; %Cv = percentage difference between the observed and predicted daily streamflow coefficients of variation.

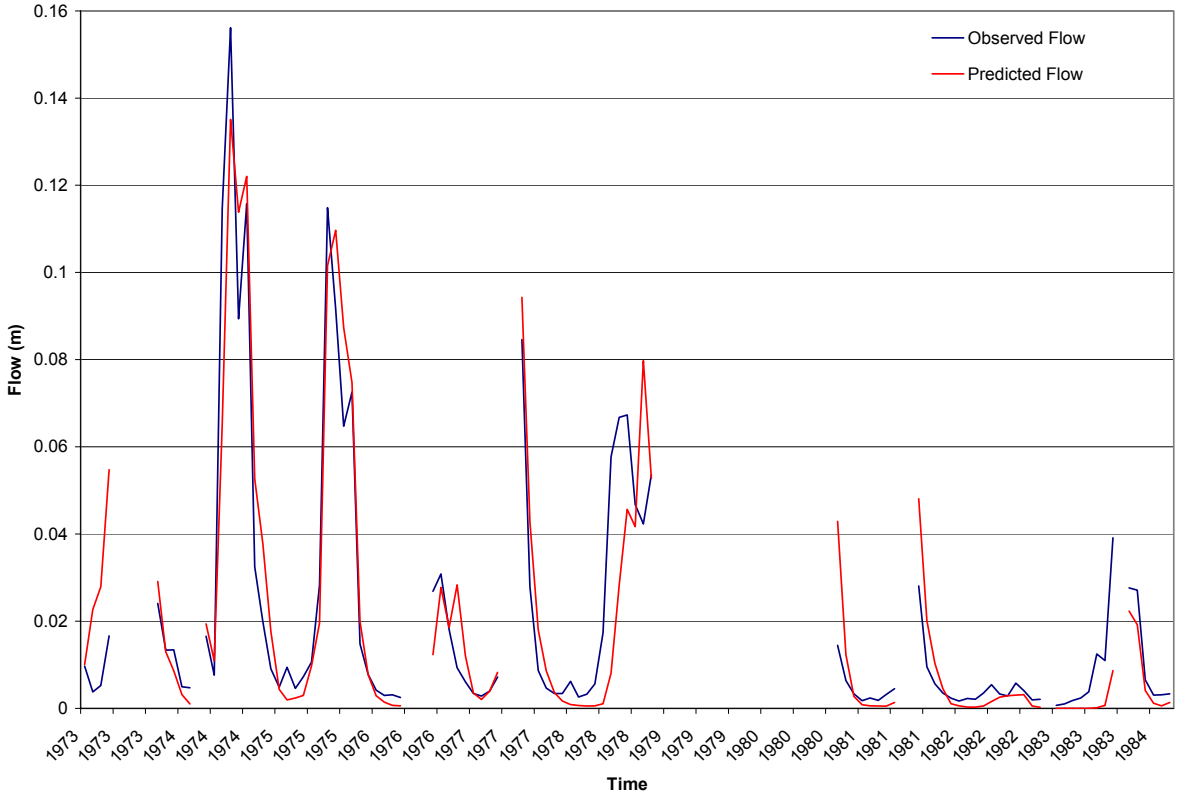

Figure 4.9. Predicted and observed total monthly flow in metres (m) for the Armstrong Creek East catchment.

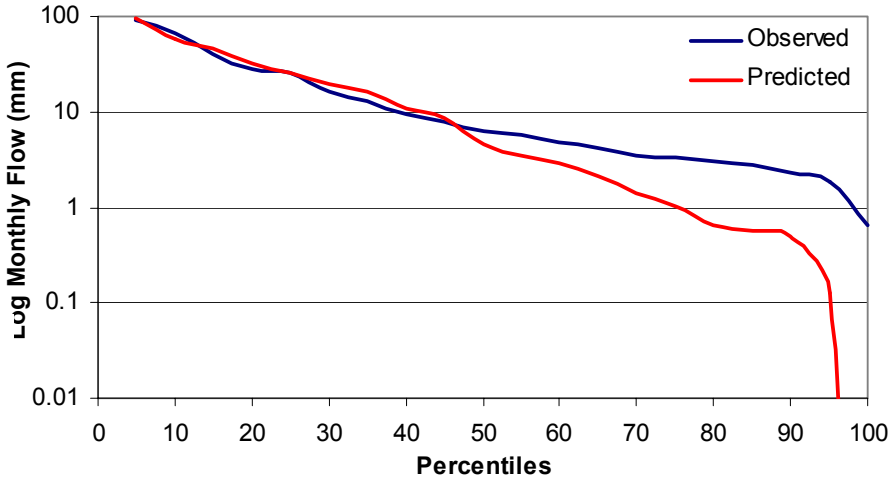

Figure 4.10. Flow duration curves for observed and predicted streamflow for the Armstrong Creek East catchment.

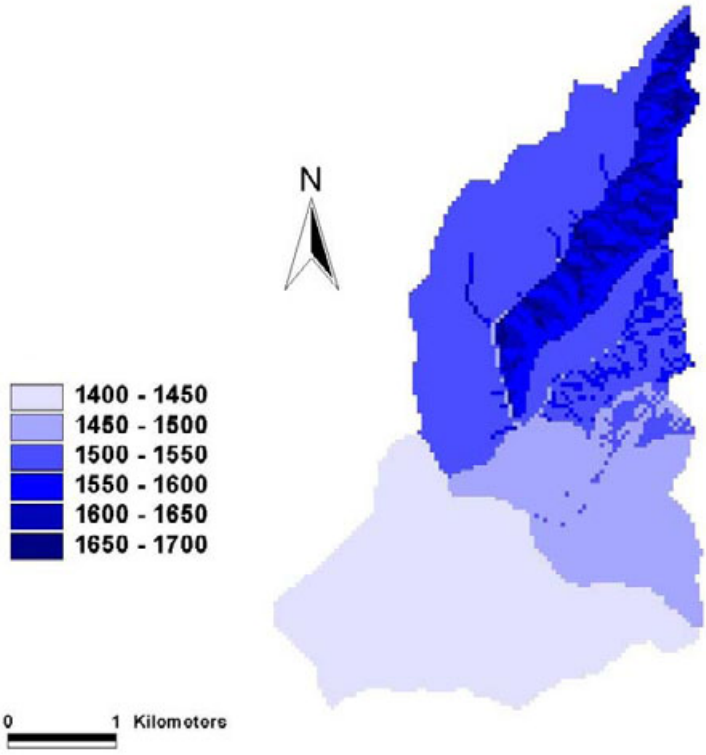

Figure 4.11. Map of mean annual precipitation (mm) (synthetic) for the Armstrong Creek East catchment for the calibration period between 1974 and 1983 (10 years) produced using the MLR precipitation mapping method described in Section 3.4.3 and model calibration.

Figure 4.12 shows a comparison between spatial maps of a) NDVI and b) Macaque derived LAI on 23 December 1988. There are general similarities between the two, with areas of higher vegetation density and higher LAI occurring in the gullies of the catchment. Also visible is the relatively low vegetation index and LAI area in the southern portion of the catchment.

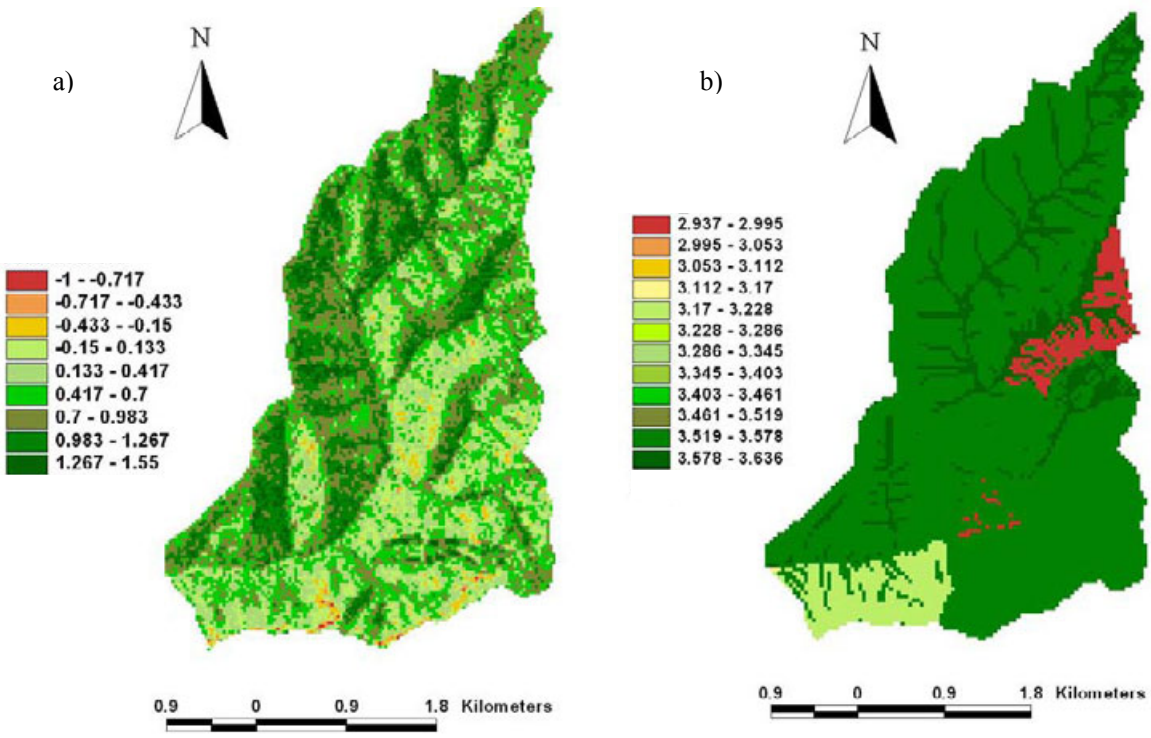

Figure 4.12. Spatial maps of a) NDVI and b) LAI for the Armstrong Creek East catchment as at December 1988.

4.8 Cement Creek

Two precipitation base stations were used (OShannassy Reservoir and Warburton) for the Cement Creek catchment. A total of 16 rainfall stations around the catchment were used to derive the precipitation coefficient maps. A list of these rainfall stations is provided in Table 4.9.

Table 4.9. List of precipitation stations used for the Cement Creek catchment. *denotes a base station.

Station name	Easting	Northing	Elevation
Balwyn Belmore Grange	384139	5818367	35.0
Black Spur	378458	5838694	567.0
Fernleigh	385475	5821127	168.0
Fernshaw	376272	5836065	210.0
Groom Hill	387594	5818226	810.0
OShannassy Reservoir*	392930	5825788	240.0
Poley Range	391180	5834155	1250.0
Starvation Ck BOM	395709	5824958	283.0
Thendara	385218	5839623	444.0
Waburton East	388408	5821167	169.0
Warburton*	383345	5820908	170.0
Warburton East (Arrabi)	388767	5822038	200.0
Mt Donna Buang	383312	5825780	1205.0
Mt Juliet	379731	5830090	1036.0
Starvation Ck MW	398368	5820908	370.0
Yarra Portal	415408	5823486	443.0

The time series of observed stream flow for the Cement Creek catchment was extremely short, extending for only 30 months. While it is possible to achieve good model performance, the period of calibration is too short (2.5 years), and any calibration parameters and subsequent analyses using these parameters would be meaningless. The calibration results are reported here in Table 4.10 for completeness, but the model is not used in any further analyses. Figure 4.13 shows the observed and predicted total flow for the entire record, and Figure 4.14 shows the flow duration curves for observed and predicted flows.

Table 4.10. Results for calibration and validation for the Cement Creek catchment.

Parameter	Calibration ALL
E	0.793
% Mean	0.26%
% SD	4.95%
% Cv	4.68%
PScalar	1.03
Hyd Grad	0.90

E = coefficient of efficiency; % Mean = percentage difference between the observed and predicted daily streamflow means; % SD = percentage difference between the observed and predicted daily streamflow standard deviations; %Cv = percentage difference between the observed and predicted daily streamflow coefficients of variation.

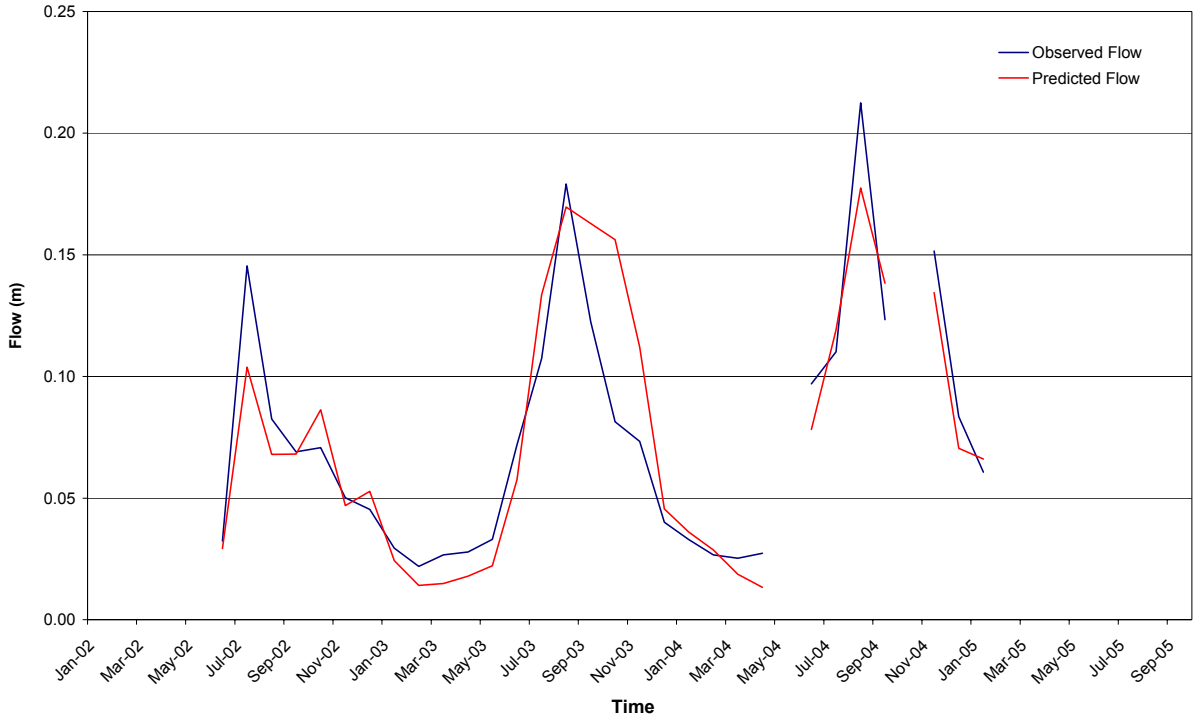

Figure 4.13. Predicted and observed total monthly flow in metres (m) for the Cement Creek catchment.

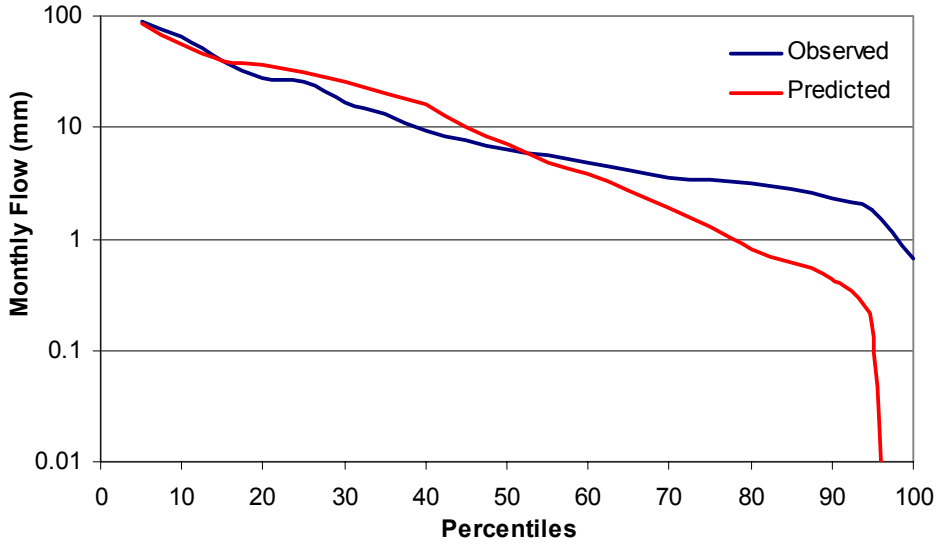

Figure 4.14. Flow duration curves for observed and predicted streamflow for the Cement Creek catchment.

4.9 McMahons Creek

Two precipitation base stations were used (at OShannassy Reservoir and Powelltown DNRE) for the McMahons Creek catchment. A total of 22 rainfall stations around the catchment were used to derive the precipitation coefficient maps. A list of these rainfall stations is provided in Table 4.11.

Table 4.11. List of precipitation stations used for the McMahons Creek and Starvartion Creek catchment. *denotes a base station.

Station name	Easting	Northing	Elevation
Ezards Old Mill Site	401780	5817809	740.0
Fernleigh	385475	5821127	168.0
Groom Hill	387594	5818226	810.0
Latrobe No 1	391571	5804563	762.0
Loch Valley	411964	5815904	561
Loch Valley Plantation	413886	5814815	558
Noojee English	412063	5806662	236.2
Noojee Forestry	411701	5805948	235.0
Noojee Slivar	409617	5804349	275.0
OShannassy Reservoir*	392930	5825788	240.0
Powelltown DNRE*	389414	5808629	189.1
Reefton	404459	5830612	616
Starvation Creek	395709	5824958	283.0
Upper Yarra Dam	402509	5829879	335.3
Walsh's Creek Station	403029	5826900	612
Warburton	383345	5820908	170.0
Warburton East	388408	5821167	168
Warburton East (Arrabi)	388767	5822038	180.0
Big Pat's Track	390312	5813180	838.0
Junction of Roads 7 & 21	413515	5825785	823
Starvation Ck	398368	5820908	370.0
Yarra Portal	415408	5823486	443.0

Values of model performance for each of the three calibration periods (two thirds) and corresponding validation period (remaining third) for the McMahons Creek catchment are listed in Table 4.12. These values of model performance for each calibration and validation period are for the single model run considered to exhibit the best model performance for each calibration period. The set of model parameters that give the best overall model performance, based on assessment of the four calibration periods, are given in Table 4.2. The overall performance was satisfactory, with E values generally above 0.60. Model performance is generally slightly lower for the non-calibration periods. Interestingly, the model had a tendency to over predict the wetter periods, and under predict the drier sequences towards the end of the record. Consequently, the selected best model run represents a compromise between the three best calibration runs. The result is that model performance as assessed by the values in Table 4.12 may not be particularly good for any individual calibration period, but provides the best achievable fit overall. Figure 4.16 shows the observed and predicted total flow for the entire record, and Figure 4.15 shows the flow duration curves for observed and predicted flows.

Figure 4.15 shows a map of the resulting predicted precipitation across the catchment from Macaque using the best calibration parameters.

Table 4.12. Results for calibration and validation for the McMahons Creek catchment.

Parameter	Calibration 1 & 2	Validation 3	Calibration 2 & 3	Validation 1	Calibration 1 & 3	Validation 2	Calibration ALL
E	0.679	0.303	0.574	0.7361	0.6738	0.5915	0.640
% Mean	0.90	-30.78	0.04	14.33	0.56	11.83	-1.71
% SD	-20.93	-24.11	-6.41	-4.41	2.37	-20.49	-10.13
% Cv	-21.63	9.64	-6.44	-16.39	1.80	-28.90	-8.57
PScalar	1.40		1.445		1.445		1.42
Hyd Grad	0.935		0.935		0.935		0.935

E = coefficient of efficiency; % Mean = percentage difference between the observed and predicted daily streamflow means; % SD = percentage difference between the observed and predicted daily streamflow standard deviations; %Cv = percentage difference between the observed and predicted daily streamflow coefficients of variation, PScalar = precipitation scalar; Hyd Grad = hydraulic gradient.

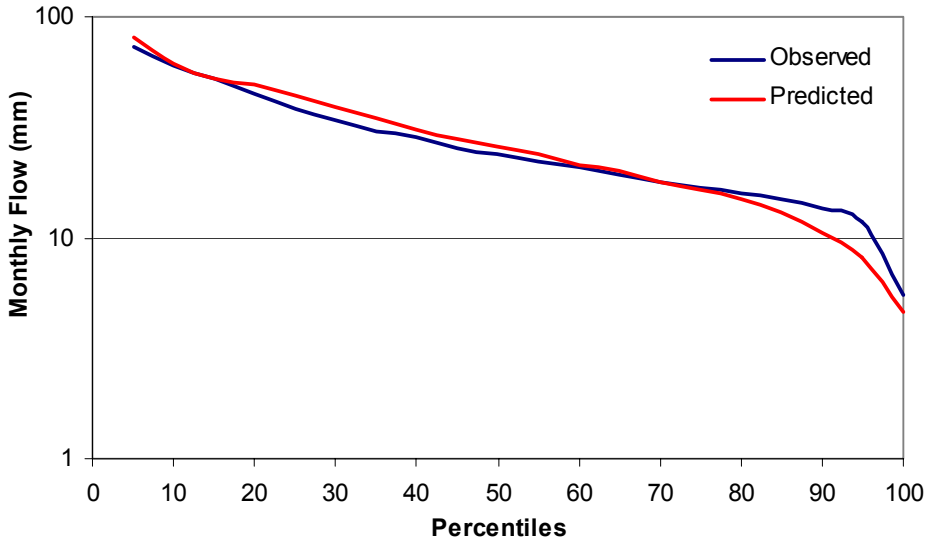

Figure 4.15. Flow duration curves for observed and predicted streamflow for the McMahons Creek catchment.

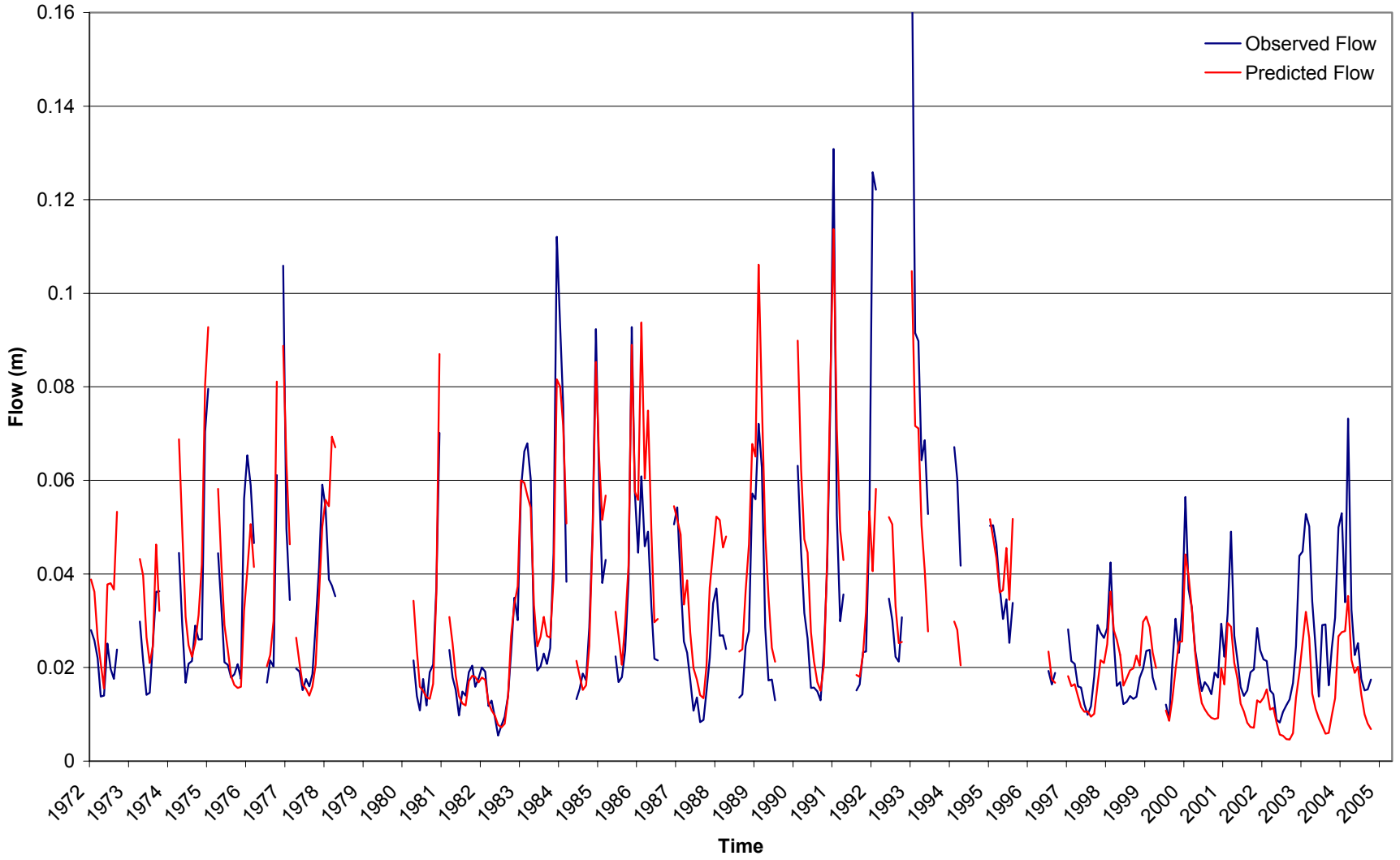

Figure 4.16. Predicted and observed total monthly flow in metres (m) for the McMahons Creek catchment.

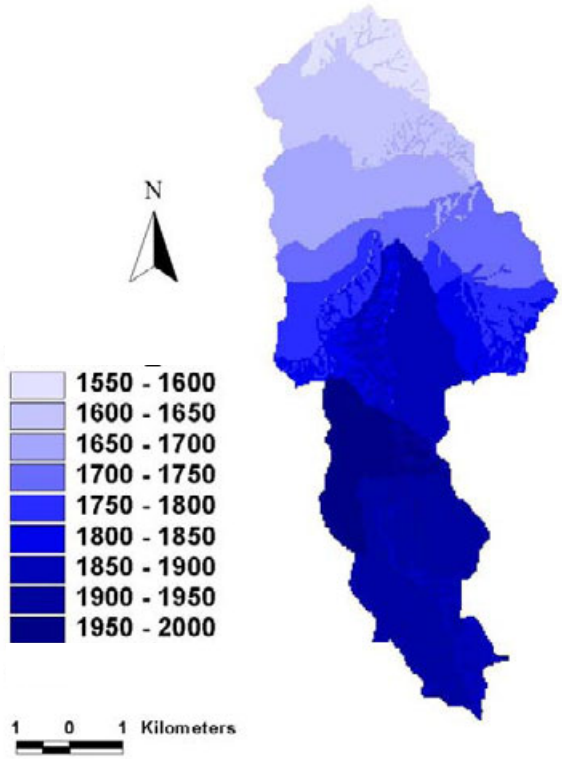

Figure 4.17. Map of mean annual precipitation (mm) (synthetic) for the McMahons Creek catchment for the calibration period between 1973 and 2004 (32 years) produced using the MLR precipitation mapping method described in Section 3.4.3 and model calibration.

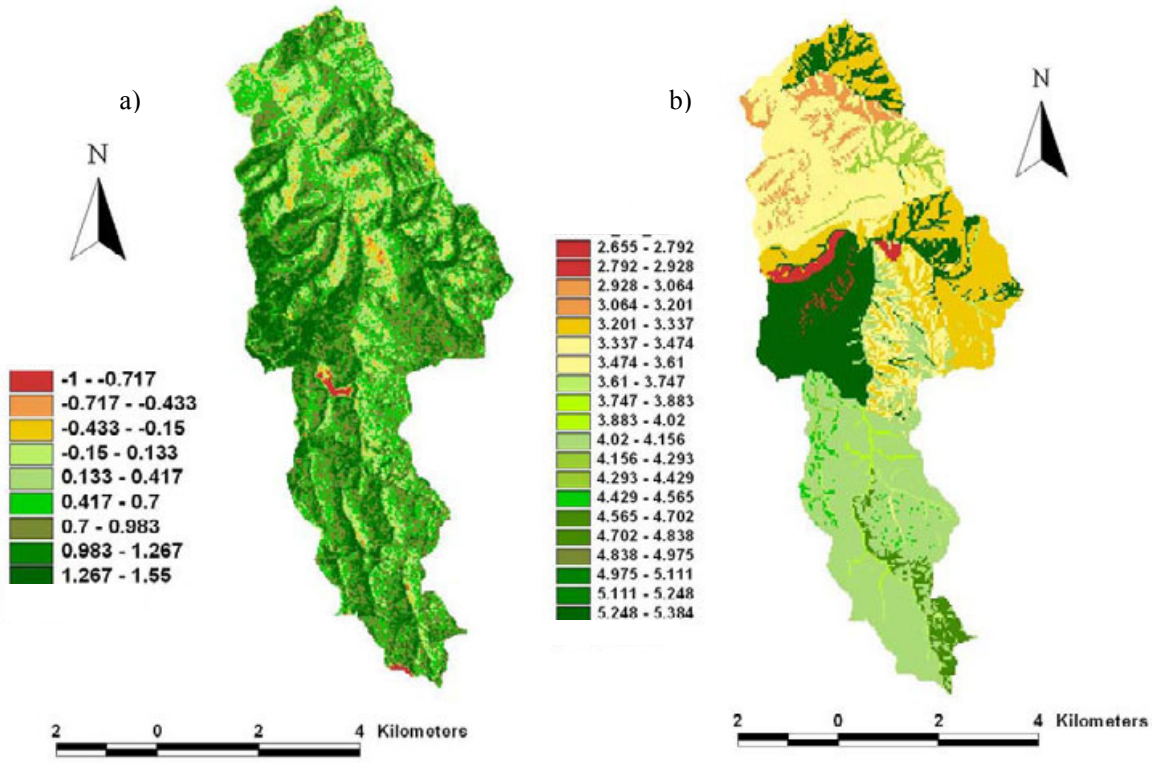

Figure 4.18. Spatial maps of a) NDVI and b) LAI for the McMahons Creek catchment as at December 1988.

Figure 4.18 shows a comparison between spatial maps of a) NDVI and for b) Macaque derived LAI on 23 December 1988. There are general similarities between the two, with areas of higher vegetation density and higher LAI occurring in the central portion along the eastern boundary of the catchment. Also visible is the relatively low vegetation index and LAI area in the northern portion of the catchment.

4.10 Starvation Creek

Two precipitation base stations were used (at OShannassy Reservoir and Powelltown DNRE) for the Starvation Creek catchment. A total of 22 rainfall stations around the catchment were used to derive the precipitation coefficient maps. These are the same stations used for the McMahons Creek catchment as well. A list of these rainfall stations is provided in Table 4.11.

Values of model performance for each of the three calibration periods (two thirds) and corresponding validation period (remaining third) for the Starvation Creek catchment are listed in Table 4.13. These values of model performance for each calibration and validation period are for the single model run considered to exhibit the best model performance for each calibration period. The set of model parameters that give the best overall model performance, based on assessment of the four calibration periods, are given in Table 4.2. The overall performance was satisfactory, with E values generally above 0.60. Model performance is generally slightly lower for the non-calibration periods. As for the McMahons Creek catchment, the model had a tendency to over predict the wetter periods, and under predict the drier sequences towards the end of the record. Therefore, the model parameters required to calibrate the model to the three calibration periods are quite different, and consequently, the selected best model run represents a compromise between the three best calibration runs. The result is that model performance as assessed by the values in Table 4.13 may not be particularly good for any individual calibration period, but provides the best achievable fit overall. Figure 4.19 shows the observed and predicted total flow for the entire record, and Figure 4.20 shows the flow duration curves for observed and predicted flows.

Figure 4.21 shows a map of the resulting predicted precipitation across the catchment from Macaque using the best calibration parameters.

Table 4.13. Results for calibration and validation for the Starvation Creek catchment.

Parameter	Calibration 1 & 2	Validation 3	Calibration 2 & 3	Validation 1	Calibration 1 & 3	Validation 2	Calibration ALL
E	0.596	0.788	0.637	0.652	0.715	0.564	0.641
% Mean	10.08	-19.10	-4.99	18.11	0.29%	4.32	1.99
% SD	-1.78	4.28	5.63	14.10	19.33	-8.98	7.86
% Cv	-10.78	29.0	11.18	-3.44	18.98	-12.75	5.76
PScalar	1.415		1.415		1.415		1.415
Hyd Grad	0.89		0.89		0.89		0.89

E = coefficient of efficiency; % Mean = percentage difference between the observed and predicted daily streamflow means; % SD = percentage difference between the observed and predicted daily streamflow standard deviations; %Cv = percentage difference between the observed and predicted daily streamflow coefficients of variation, PScalar = precipitation scalar; Hyd Grad = hydraulic gradient.

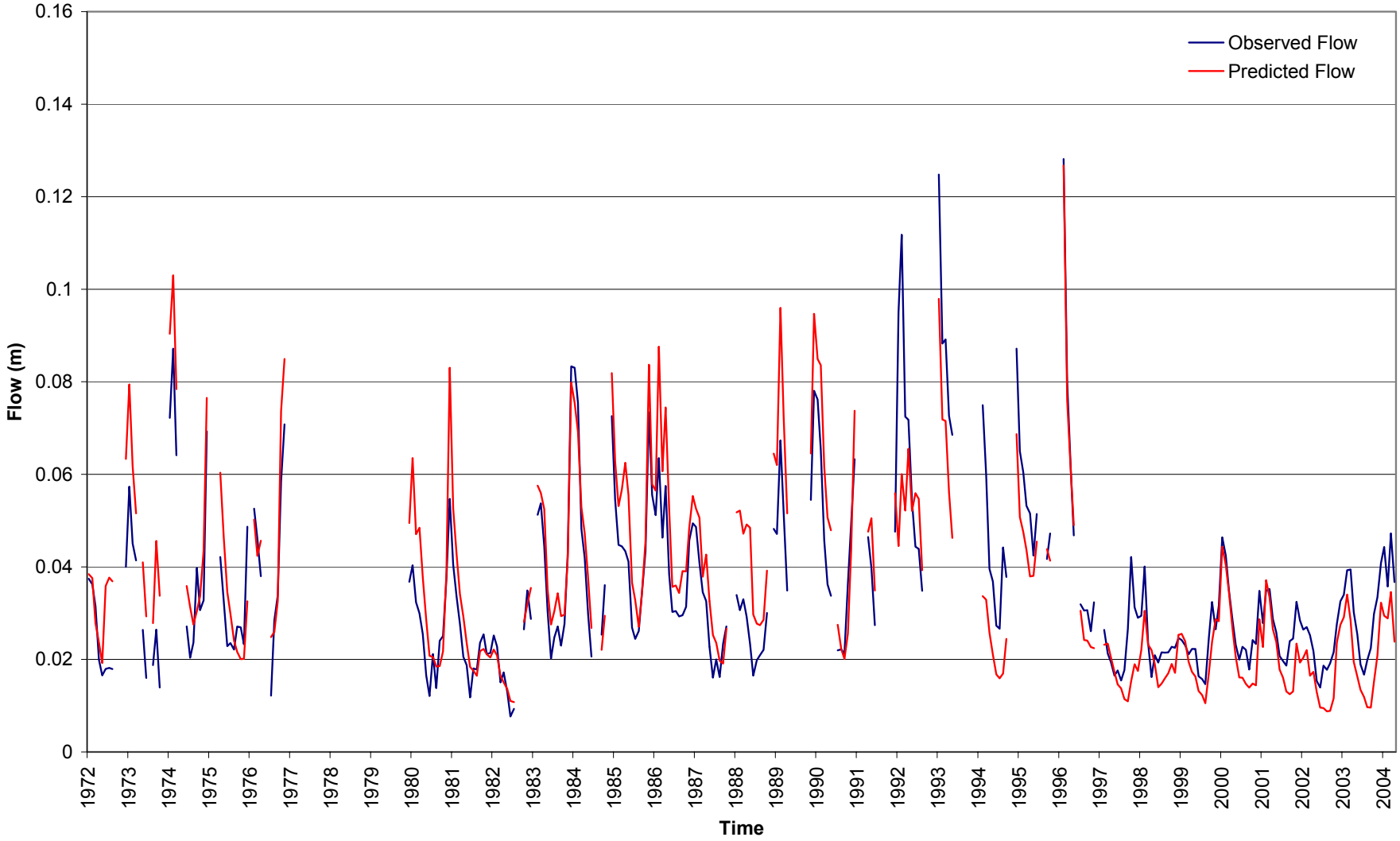

Figure 4.19. Predicted and observed total monthly flow in metres (m) for the Starvation Creek catchment.

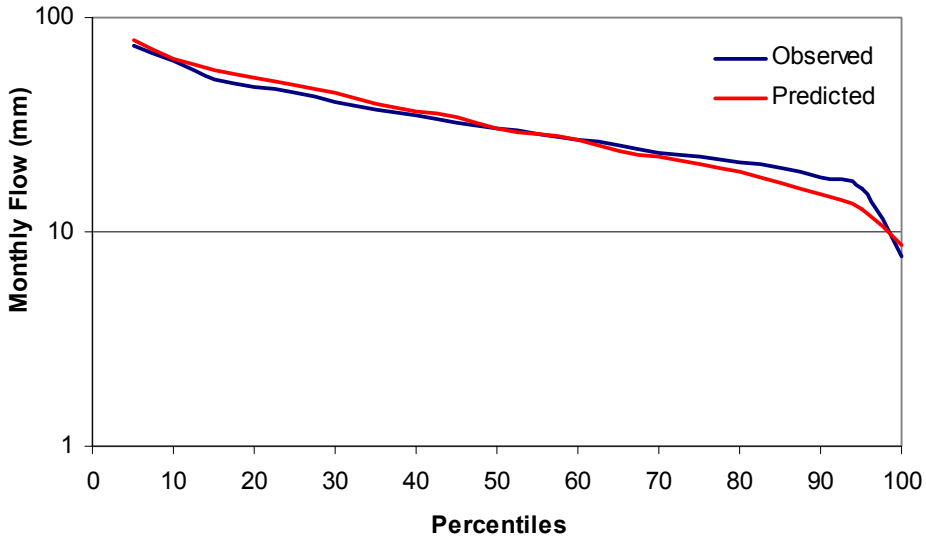

Figure 4.20. Flow duration curves for observed and predicted streamflow for the Starvation Creek catchment.

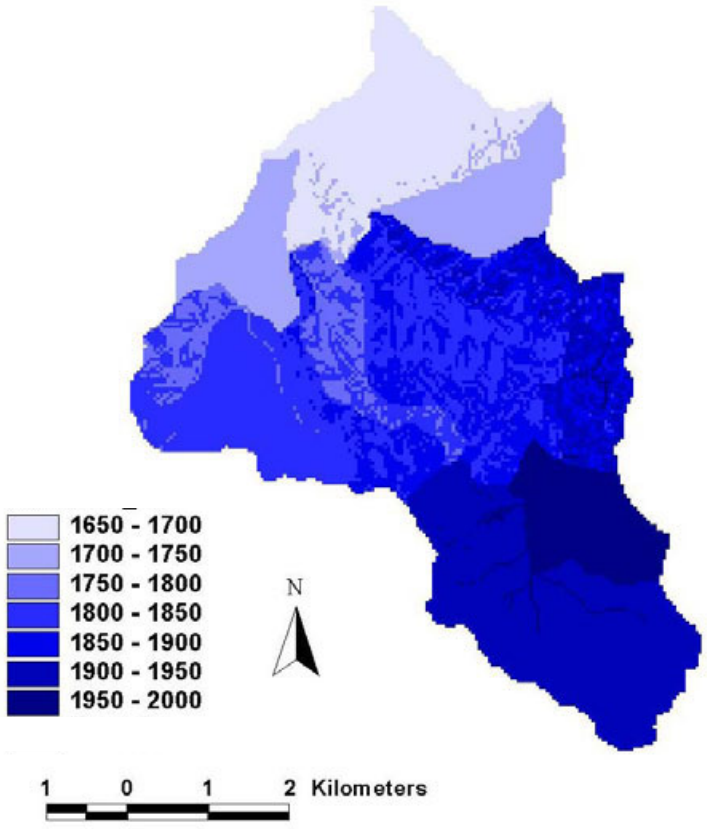

Figure 4.21. Map of mean annual precipitation (mm) (synthetic) for the Starvation Creek catchment for the calibration period between 1973 and 2004 (32 years) produced using the MLR precipitation mapping method described in Section 3.4.3 and model calibration.

Figure 4.22 shows a comparison between spatial maps of a) NDVI and b) Macaque derived LAI on 23 December 1988. There are general similarities between the two, with areas of higher vegetation density and higher LAI occurring in the central west of the catchment. Also visible is the relatively low vegetation index and LAI area in the northern portion of the catchment.

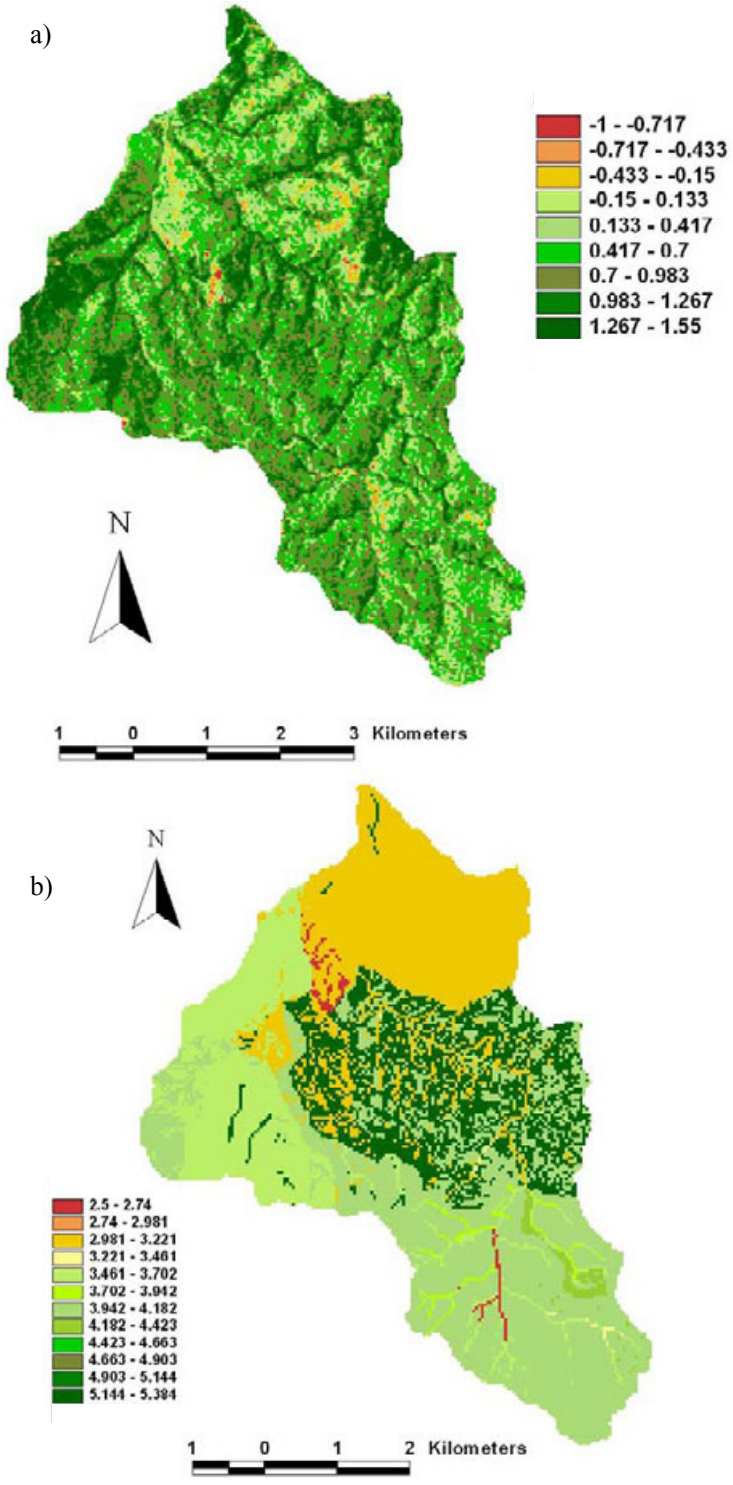

Figure 4.22. Spatial maps of a) NDVI and b) LAI for the Starvation Creek catchment as at 23 December 1988.

4.11 Tarago

Two precipitation base stations were used (at Powelltown DNRE and Jindivik PO) for the Tarago catchment. A total of 23 rainfall stations in and around the catchment were used to derive the precipitation coefficient maps. A list of these rainfall stations is provided in Table 4.14.

Table 4.14. List of precipitation stations used for the Tarago catchment. *denotes a base station.

Station name	Easting	Northing	Elevation
Buln Buln	409861	5782224	195
Gilderoy	385706	5804484	402
Jindivick PO (Post Office)*	402432	5791161	250
Jindivick North	404464	5792328	237
Labertouche	393233	5787750	65
Latrobe No 1	391571	5804563	762
Neerim	412142	5799261	377
Neerim Junction	409196	5801082	446
Neerim South	407988	5791259	254
Nojee	412082	5804809	244
Noojee English	412063	5806662	236
Noojee Forestry	411701	5805948	235
Noojee Slivar	409617	5804349	275
Powelltown DNRE*	389414	5808629	189
Tarago Reservoir	406935	5791225	180
Bunyip@Headworks	389463	5799785	125
Drewsdene	409216	5799229	422
Drouin West	397398	5783764	71
Mt Duffy	415112	5805229	1029
Neerim East	416116	5792179	300
Neerim North	409175	5802924	480
Noojee North	412082	5804809	342
Tonimbuk	382514	5795282	150

Values of model performance for each of the three calibration periods (two thirds) and corresponding validation period (remaining third) for the Tarago catchment are listed in Table 4.15. These values of model performance for each calibration and validation period are for the single model run considered to exhibit the best model performance for each calibration period. The set of model parameters that give the best overall model performance, based on assessment of the four calibration periods, are given in Table 4.2. The overall performance was satisfactory, with E values generally above 0.65. Model performance is generally slightly lower for the non-calibration periods.

Figure 4.24 shows the observed and predicted total flow for the entire record, and Figure 4.23 shows the flow duration curves for observed and predicted flows. Figure 4.25 shows a map of the resulting predicted precipitation across the catchment from Macaque using the best calibration parameters.

The streamflow record suitable for calibration consists of two periods, one from 1944 until 1963 and another from 1996 until 2005. The reason for this is that water extraction commenced upstream of the calibration point at the Pedersen Wier in December 1963. While streamflow data was available at the

calibration point from 1944 until 2005, data from extractions at the Pedersen Weir were not available until July 1996. So the complete water balance for the catchment between 1963 and 1996 is not available. It was interesting to note that, during 1963 and 1996, when no flow data is available from the Pedersen Weir to be added to the flow at Tarago River at Neerim for calibration, that the predicted flow was clearly higher, as expected (Figure 4.24).

The calibration streamflow record is characterised by a relatively wet period between 1944 and 1963, and a very dry period between 1996 and 2005 (Figure 4.24). However, neither of the two base stations (at Powelltown and at Jindivik)) used to drive the estimated precipitation across the catchment appeared to have relatively higher rainfall in the earlier, wetter period. These rainfall stations are located 7.5km to the north west and 0.5 km to the south of the catchment respectively. It is possible that rainfall at the two base stations did not capture the relatively higher rainfall that occurred across the catchment in the wettest period between 1952-56. Alternatively, it is possible that systematic errors have led to overestimation of actual streamflows in the earlier part of the streamflow record.

Consequently, the model tended to under predict during the period of higher flows between 1944 and 1963 and over predict the relatively low flows between 1996 and 2005. Model parameters required to calibrate the model to the three calibration periods are quite different, and consequently, the selected best model run represents a compromise between the three best calibration runs. Given that the effects of climate change are more likely to result in lower flows in the future, it was decided that more weight should be given to calibrating the model for the more recent lower flow periods. The result is that model performance as assessed by the values in Table 4.15 may not be particularly good for any individual calibration period, but provides the best achievable fit overall.

The Tarago is the only catchment within this study to have any sizeable portion (20%) of grassland within it. The subcatchment used for calibration contained about 12% of grassland. This presents some complexities when calibrating Macaque for this catchment. The NDVI image (Figure 4.26a) indicates that the area classified as grassland consists of agricultural areas that are unirrigated or irrigated. This area represents a heterogenous landscape with large differences in NDVI, indicative of large differences in leaf area index for grassland. Another image of NDVI taken in March 2001 (not shown here) indicates that there is substantial temporal variation in the agricultural region. Several areas (paddocks) that showed high values of NDVI in December 1988 at the start of summer, showed low values at the end of summer in March 2001. Macaque is unable to represent the spatial and temporal variation evident in the agricultural region of the Tarago catchment. The water yield resulting from this landuse is likely to be more variable than the forested areas in the catchment, and therefore likely to be subject to greater errors when predicting yields from this vegetation type.

The fact that irrigation occurs in the agricultural parts of this catchment may lead to changes in the water balance spatially, temporally and in total volume. If water used for irrigation is derived from outside the catchment, then the rainfall required to increase yield will result in an over estimation of the precipitation scalar.

Table 4.15. Results for calibration and validation for the Tarago catchment.

Parameter	Calibration 1 & 2	Validation 3	Calibration 2 & 3	Validation 1	Calibration 1 & 3	Validation 2	Calibration ALL
E	0.761	0.328	0.660	0.723	0.688	0.615	0.688
% Mean	-1.72%	43.28%	0.19%	-5.97%	-0.20%	-21.78%	-1.01%
% SD	1.14%	51.62%	-1.03%	-4.38%	-3.96%	-5.57%	-1.33%
% Cv	2.91%	5.82%	-1.22%	1.69%	-3.77%	20.72%	-0.32%
PScalar	1.46		1.42		1.395		1.435
Hyd Grad	0.89		0.90		0.904		0.901

E = coefficient of efficiency; % Mean = percentage difference between the observed and predicted daily streamflow means; % SD = percentage difference between the observed and predicted daily streamflow standard deviations; %Cv = percentage difference between the observed and predicted daily streamflow coefficients of variation, PScalar = precipitation scalar; Hyd Grad = hydraulic gradient.

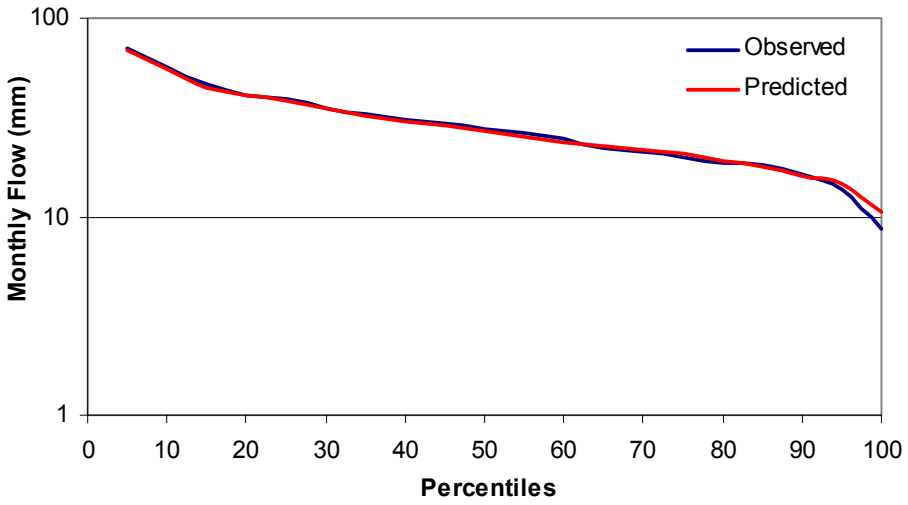

Figure 4.23. Flow duration curves for observed and predicted streamflow for the Tarago catchment at Tarago River at Neerim.

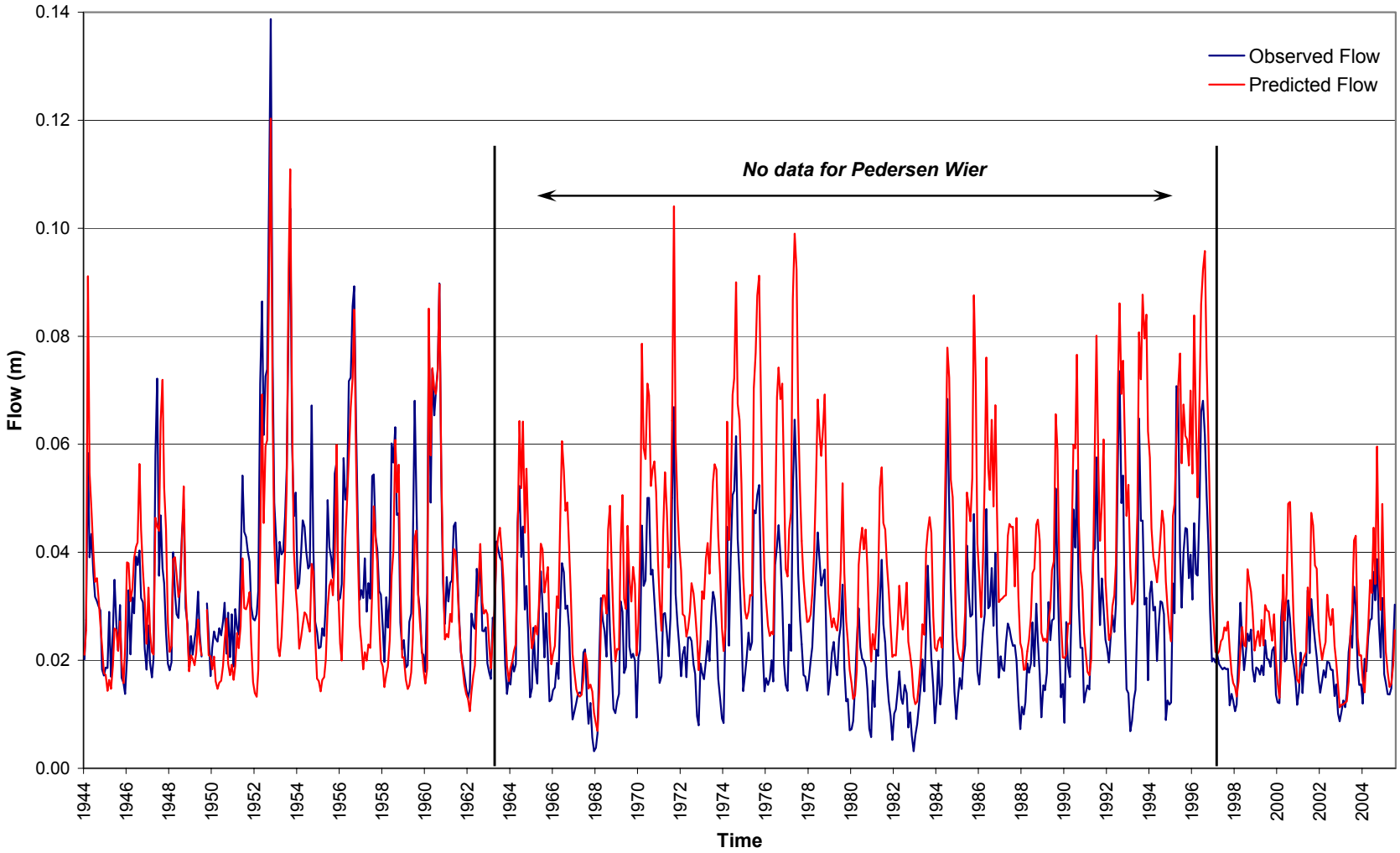

Figure 4.24. Predicted and observed total monthly flow for the Tarago catchment.

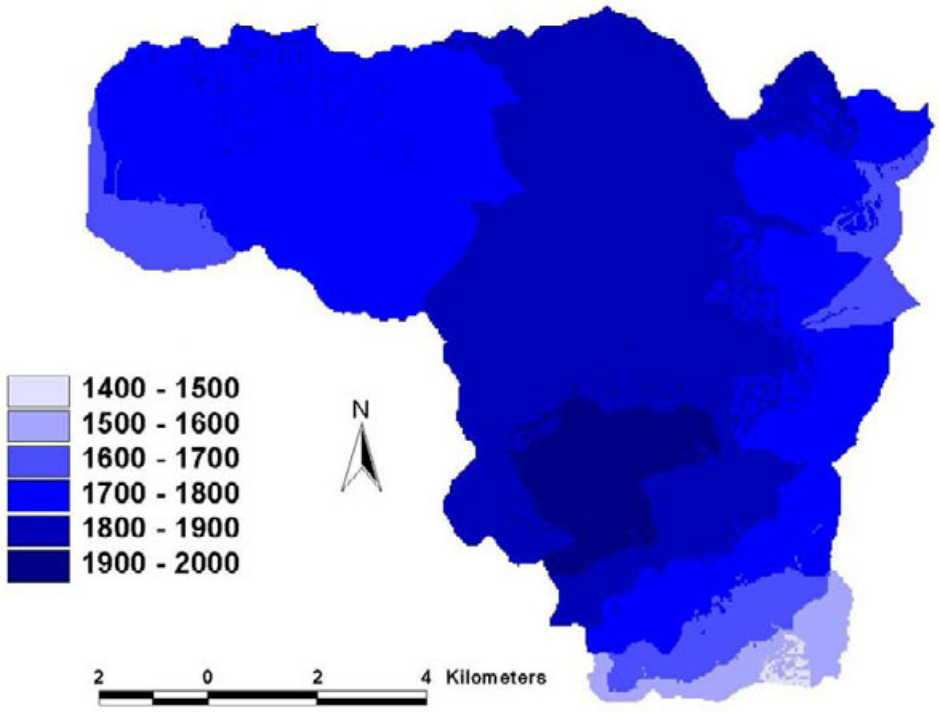

Figure 4.25. Map of mean annual precipitation (mm) (synthetic) for the Tarago catchment for the calibration period between 1944 and 2004 (61 years) produced using the MLR precipitation mapping method described in Section 3.4.3 and model calibration.

Figure 4.26 shows a comparison between spatial maps of a) NDVI and b) Macaque derived LAI on 23 December 1988. The agricultural areas, along with their relatively large variation in NDVI (and therefore LAI) is clearly visible along the eastern portion of the catchment. It is evident that values for LAI in the agricultural may be both lower and higher (depending on whether they represent unirrigated or irrigated land respectively) than those of the native forest within the catchment.

There are general similarities between the two, with areas of higher vegetation density and higher LAI occurring in the central west of the catchment. Also visible is the relatively low vegetation index and LAI area in the northern portion of the catchment, and in isolated small areas in the southern part of the catchment.

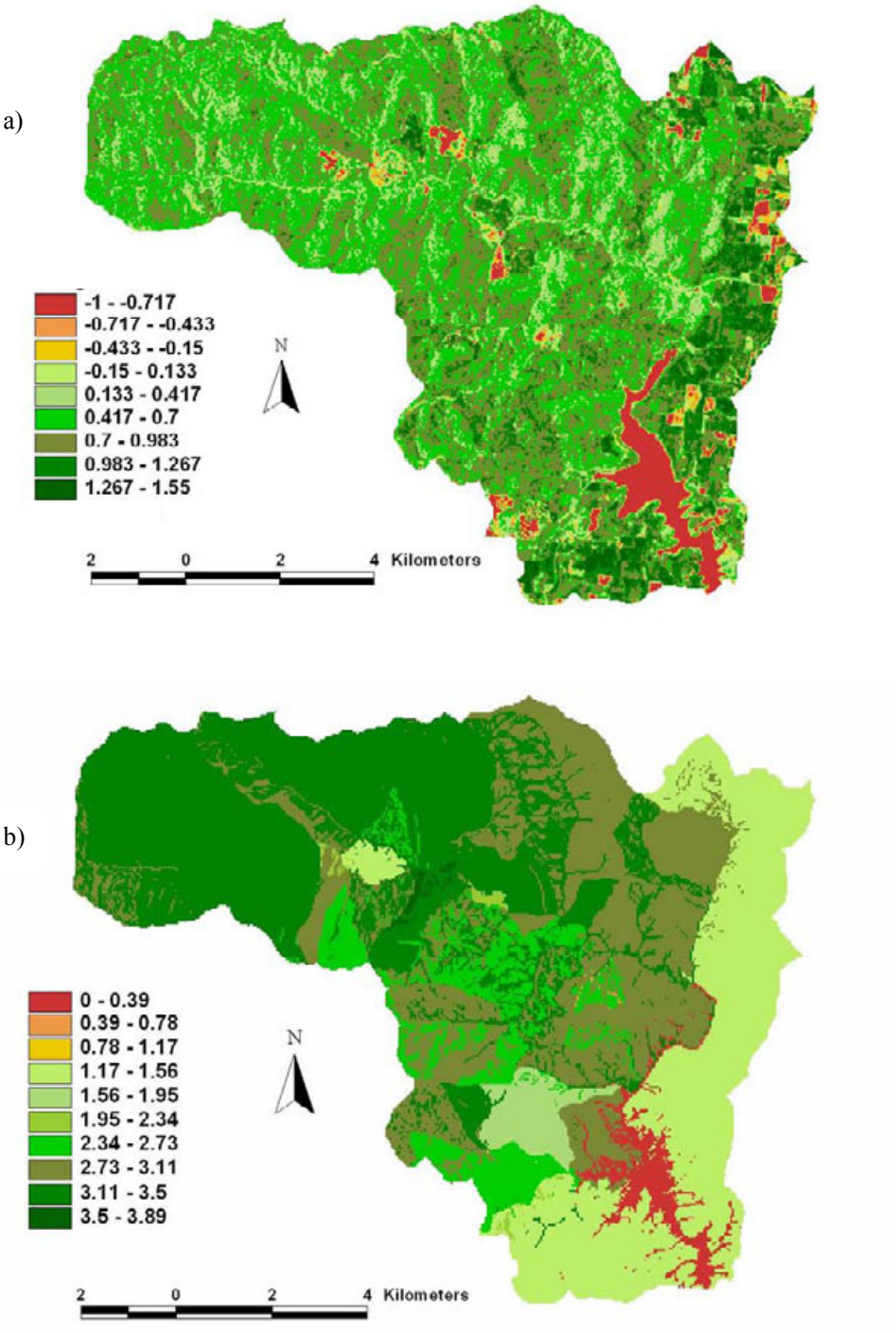

Figure 4.26. Spatial maps of a) NDVI and b) LAI for the Tarago catchment as at 23 December 1988.

4.12 Bunyip

Two precipitation base stations were used (at Powelltown DNRE and Labertouche) for the Bunyip catchment. A total of 21 rainfall stations around the catchment were used to derive the precipitation coefficient maps. A list of these rainfall stations is provided in Table 4.14.

Table 4.16. List of precipitation stations used for the Bunyip catchment. *denotes a base station.

Station name	Easting	Northing	Elevation
Balwyn Belmore Grange	384139	5818367	35.0
Beenak BOM	376914	5804356	609.6
Gembrook	374071	5798764	310.9
Gilderoy	385706	5804484	402
Gladysdale	381509	5810717	366.0
Groom Hill	387594	5818226	810
Hazeldene A	378355	5806231	292
Hezeldene B	382726	5808137	335.3
Jindivick PO (Post Office)	402432	5791161	250.0
Jindivick North	404464	5792328	237
Labertouche*	393233	5787750	65.0
Latrobe No 1	391571	5804563	762.0
Neerim Junction	409196	5801082	446
Powelltown DNRE*	389414	5808629	189.1
Tomahawk Valley	378465	5798830	290
Yarra Junction Waterworks	382620	5815538	231.0
Beenak -RG MW	377010	5805590	283
Big Pat's Track	390312	5813180	838.0
Bunyip@Headworks	389463	5799785	125
Drouin West	397398	5783764	71.0
Tonimbuk	382514	5795282	150.0

Values of model performance for each of the three calibration periods (two thirds) and corresponding validation period (remaining third) for the Bunyip catchment are listed in Table 4.17. These values of model performance for each calibration and validation period are for the single model run considered to exhibit the best model performance for each calibration period. The set of model parameters that give the best overall, model performance, based on assessment of the four calibration periods, are given in Table 4.2.

The period of available streamflow data for calibration extended from 1948 until 1987. While streamflow data at the calibration point exists to 2005, water extracted via the Bunyip Main Race (BMR) has not been fully accounted for from 1987 onwards, and therefore a complete record of streamflow after this time is not available.

The calibration streamflow record is characterised by a relatively wet period between 1950 and 1960 (Figure 4.27). However, neither of the two base stations (at Powelltown and at Labertouche) used to drive the precipitation across the catchment appeared to have relatively higher rainfall during the wetter period between 1950-60. It is possible that rainfall at the two base stations did not capture the relatively higher

rainfall that occurred across the catchment particularly in this wet period. Alternatively, it is possible that systematic errors have led to over estimation of actual streamflow in the earlier part of the streamflow record.

The model tended to under predict during the period of higher flows between 1950 and 1960 and over predict the relatively low flows later in the calibration period. Model parameters required to calibrate the model to the three calibration periods are quite different, and consequently, the selected best model run represents a compromise between the three best calibration runs. Given that the effects of climate change are more likely to result in lower flows in the future, it was decided that more weight should be given to calibrating the model for the more recent lower flow periods. The resulting model performance as assessed by the values in Table 4.13 may not be particularly good for any individual calibration period, but provides the best achievable fit overall. The corresponding model parameters are given in Table 4.2. The overall performance was satisfactory, but some E values were below 0.50. Model performance is generally slightly lower for the non-calibration periods.

Figure 4.24 shows the observed and predicted total flow for the entire record, and Figure 4.23 shows the flow duration curves for observed and predicted flows. Figure 4.29 shows a map of the resulting predicted precipitation across the catchment from Macaque using the best calibration parameters.

Table 4.17. Results for calibration and validation for the Bunyip catchment.

Parameter	Calibration 1 & 2	Validation 3	Calibration 2 & 3	Validation 1	Calibration 1 & 3	Validation 2	Calibration ALL
E	**0.563**	**-0.940**	**0.568**	**-0.0791**	**0.289**	**0.594**	**0.357**
% Mean	-0.77%	51.07%	1.12%	-39.38%	-3.43%	-27.34%	-2.45%
% SD	-0.30%	43.78%	2.03%	-36.19%	-3.54%	-9.96%	-0.97%
% Cv	0.48%	-4.82%	0.89%	5.26%	-0.11%	23.91%	1.51%
PScalar	1.59		1.485		1.53		1.53
Hyd Grad	0.85		0.80		0.96		0.96

E = coefficient of efficiency; % Mean = percentage difference between the observed and predicted daily streamflow means; % SD = percentage difference between the observed and predicted daily streamflow standard deviations; %Cv = percentage difference between the observed and predicted daily streamflow coefficients of variation, PScalar = precipitation scalar; Hyd Grad = hydraulic gradient.

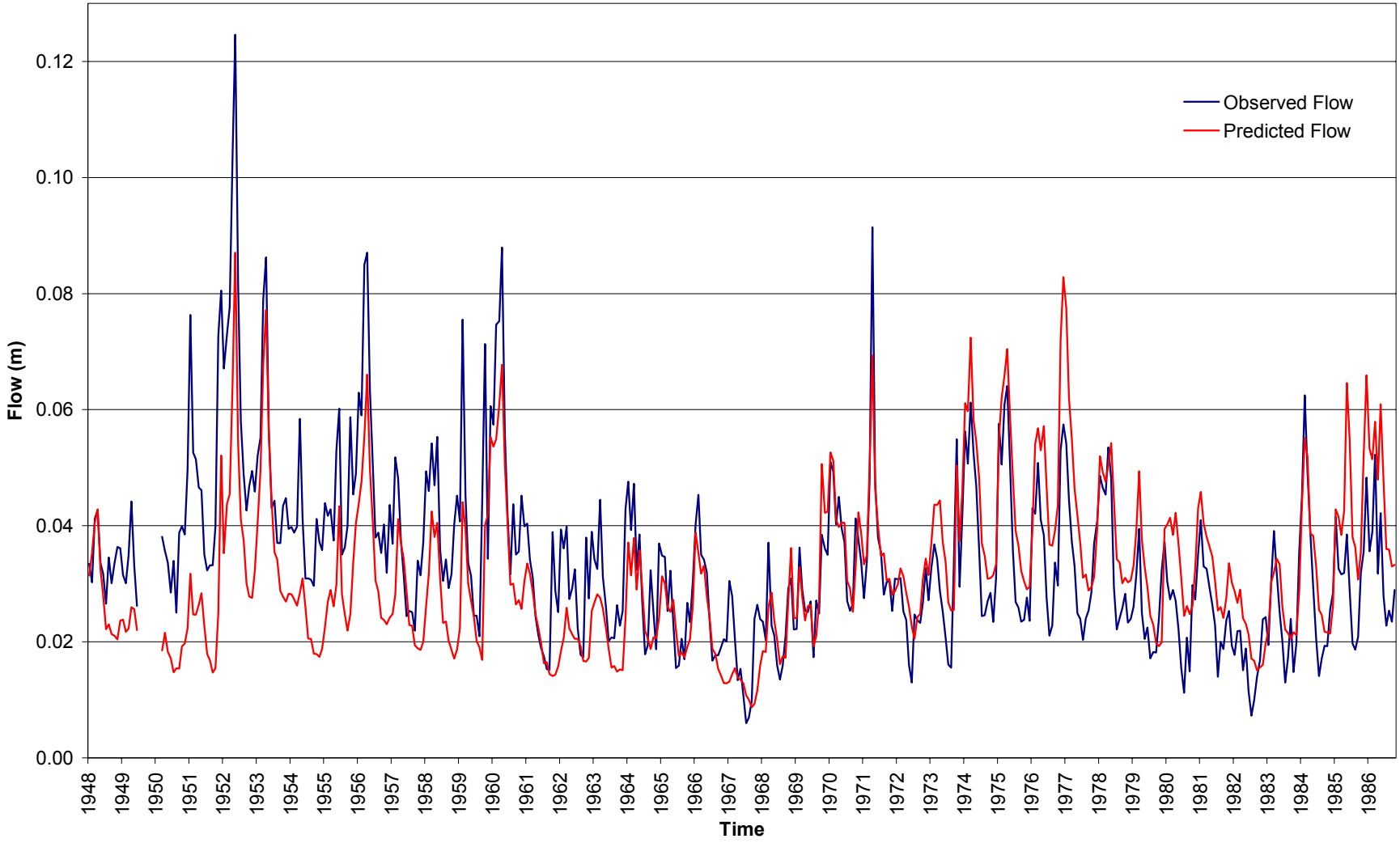

Figure 4.27. Predicted and observed total monthly flow in metres (m) for the Bunyip catchment.

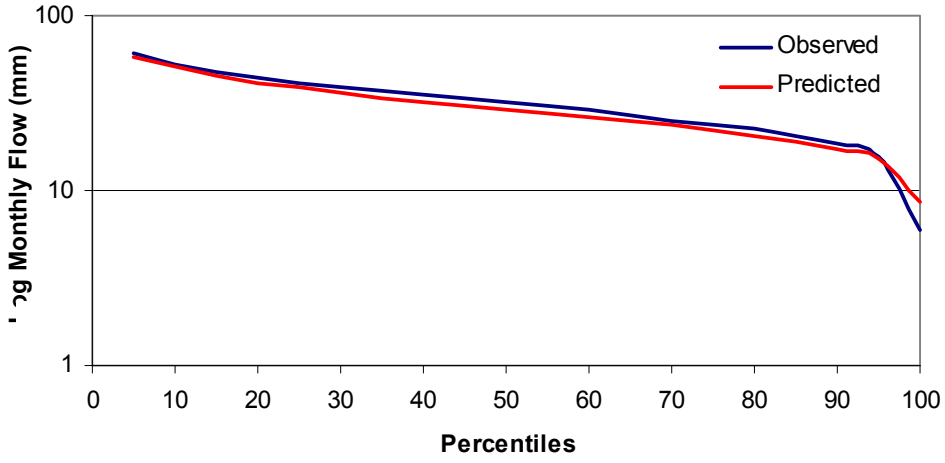

Figure 4.28. Flow duration curves for observed and predicted streamflow for the Bunyip catchment.

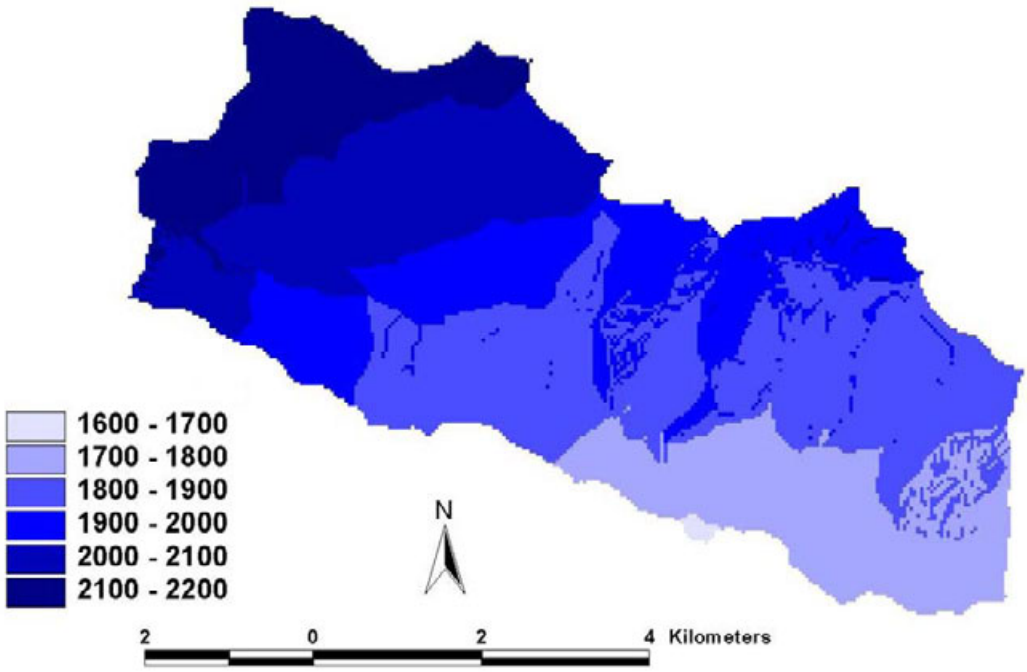

Figure 4.29. Map of mean annual precipitation (mm) (synthetic) for the Bunyip catchment for the calibration period between 1948 and 1987 (40 years) produced using the MLR precipitation mapping method described in Section 3.4.3 and model calibration.

Figure 4.30 shows a comparison between spatial maps of a) NDVI and b) Macaque derived LAI on 23 December 1988. There are general similarities between the two, with low vegetation index areas along the northern boundary of the catchment corresponding to a general area of lower LAI.

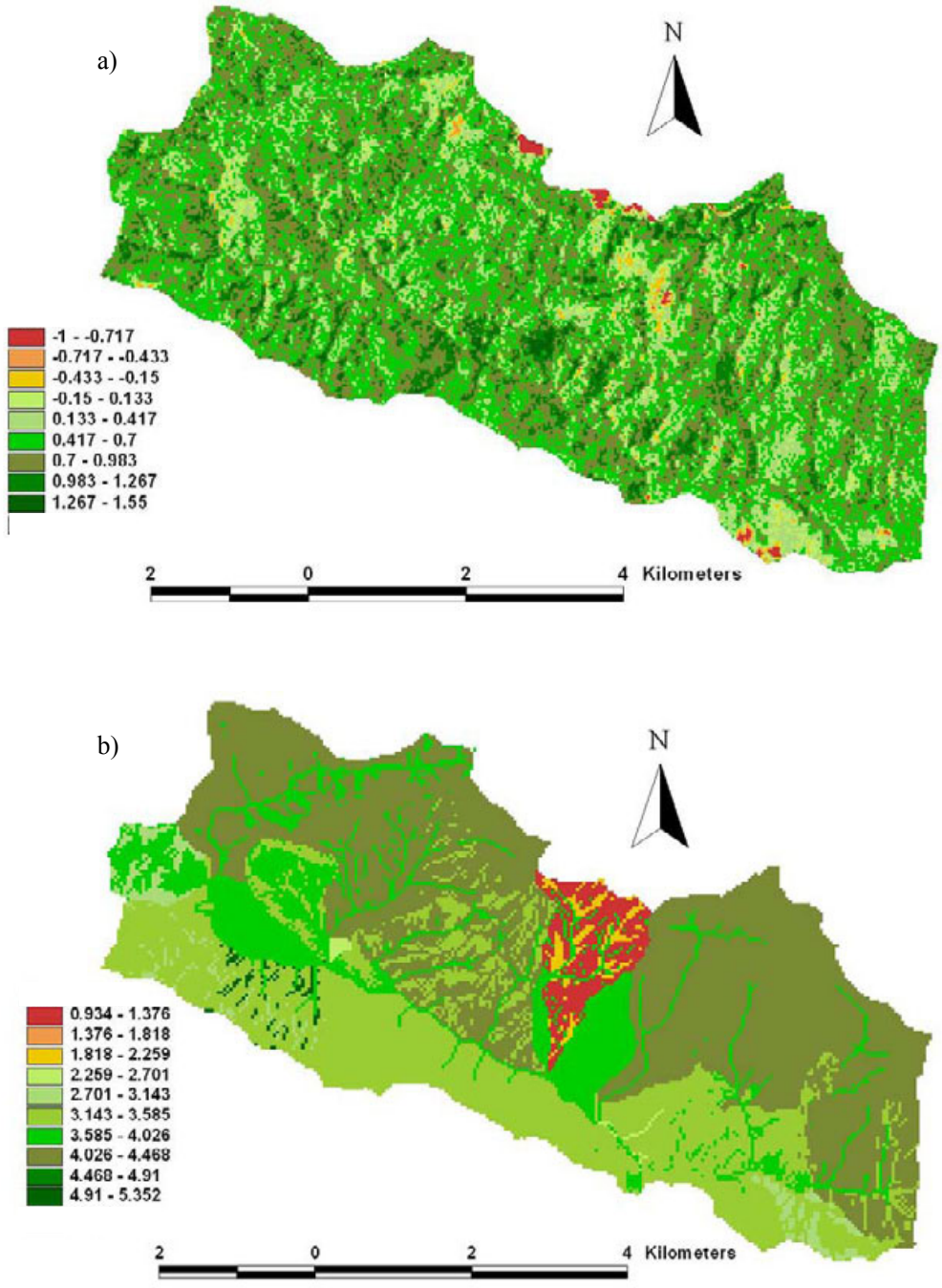

Figure 4.30. Spatial maps of a) NDVI and b) LAI for the Bunyip catchment as at 23 December 1988.

4.13 Summary

In general, the calibrated values of the coefficient of efficiency, and changes in mean, standard deviation and coefficient of variation indicate that Macaque is modelling most of the catchments satisfactorily and in most cases quite well.

The model performance tended to improve as the catchment size increased, a trend also noted by Peel *et al*. (2000). Furthermore, the value for the ratio of the hydraulic to surface gradient also increased with increasing catchment size. The only exceptions to this trend were the Tarago and Bunyip catchments, where these two catchments were not the smallest catchments, but clearly had the lowest value for this parameter to produce a good model fit. Decreasing the hydraulic to surface gradient effectively simulates a deeper watertable, and results in less variable streamflow. In the case of the Tarago catchment, it is possible that construction of the observed streamflow record by adding extractions upstream on a monthly basis has led to a decrease in variability that otherwise would have naturally occurred.

5. Sensitivity analysis

5.1 Introduction

Macaque uses a set of curves that relate the leaf area index (LAI) of a forest species to the age of that forest species, and then uses other curves that relate maximum leaf conductance to age for all eucalypt species. These curves were derived from direct measurements as well as allometric and remote sensing data throughout the Maroondah region in southern Victoria. This introduces uncertainty in the accurate representation of these relationships in other catchments.

A sensitivity analysis allows the quantification of the uncertainty in the calibrated model caused by uncertainty in the estimates of vegetation parameters. A sensitivity analysis was conducted on the Thomson catchment to investigate the impact of uncertainty in LAI and conductance on flow and total ET. In turn, values for LAI, and conductance were increased and then decreased by 10%, and the model outputs were examined.

These changes in LAI and conductance were undertaken on the calibrated model of the Thomson (which incorporates natural interannual climate variability) and then also on a long-term model used to generate the yield curves (as described in Section 7) which has no interannual climate variability. A year of actual climate record (rainfall and temperature) for the Thomson catchment was selected be representative of the average annual longer term rainfall. The representative year of rainfall was repeated to create a 300-year rainfall record. The resulting synthetic 300-year sequence had no inter-annual variability. This simulation used the same vegetation distribution map used in the calibration simulations. The vegetation was 270 years old at the start of the simulation, allowed to grow for 10 years, then the whole catchment was disturbed, and vegetation allowed to (re)grow for a further 230 years.

Simulations using a variable climate could then be compared to those which used a climate with no interannual variability. The effect of climate variability on the sensitivity of the model to changes in LAI and conductance could then also be examined.

5.2 Sensitiviy to the LAI with age relationship

To investigate the model sensitivity to changes in LAI, the maximum and long term values for LAI (where the curve by Watson (1999) is used), and the 'constant' LAI (for all the remaining vegetation types), were all increased and then decreased by 10%. The values for LAI used in these simulations are provided in Table 5.1. The resulting changes in actual LAI, total flow and total ET were then examined.

Table 5.1. Values for LAI used in the sensitivity analysis.

Forest type	LAI curve type	Maximum LAI (Default)	Long term LAI (Default)	Maximum LAI +10%	Long term LAI +10%	Maximum LAI -10%	Long term LAI -10%
E. regnans	Watson (1999)[1]	6.0	3.5	6.600	3.850	5.400	3.150
E. nitens	Watson (1999)[1]	6.0	3.5	6.600	3.850	5.400	3.150
E. delegatensis	Watson (1999)[2]	5.7	3.2	6.270	3.520	5.130	2.880
Acacia dealbata	Constant*	3.907	3.907	4.298	4.298	3.516	3.516
E. pauciflora	Constant*	2.5	2.5	2.750	2.750	2.250	2.250
E. sieberi	Constant*	2.937	2.937	3.231	3.231	2.643	2.643
Mixed spp.	Constant*	3.564	3.564	3.920	3.920	3.208	3.208
Rainforest	Constant*	3.771	3.771	4.148	4.148	3.394	3.394
Heath	Constant*	2.5	2.5	2.750	2.750	2.250	2.250
Leptospermum spp.	Constant*	3.353	3.353	3.688	3.688	3.018	3.018
Grassland	Constant*	1.5	1.5	1.650	1.650	1.350	1.350
'Not vegetated'	Constant*	3.153	3.153	3.468	3.468	2.838	2.838

* Constant after first 5 to 10 years after establishment; [1]Watson (1999), Equation 8.45; [2]Watson (1999), Equation 8.45. Same as [1] but with LAI lower by 0.3; [3]Watson (1999), Equation 11.1.

Changing LAI parameters by 10% led to a similar change (9.55%) in total projected LAI calculated by Macaque in the simulations with interannual climate variability (Table 5.2). This was comprised of changes to canopy LAI of 5.37% and changes to understorey LAI of 14.87%. An increase in total LAI of 9.55% led to an increase in total ET of +4.13%, and a corresponding decrease in total flow of -10.69%.

Table 5.2. Percentage change of model outputs to changes in LAI for the calibration simulation with interannual climate variability.

	Change in LAI parameters			
	+10%		-10%	
	ΔTotal%	ΔSD%	ΔTotal%	ΔSD%
Total LAI	+9.55	+9.54	-9.55	-9.49
Canopy LAI	+5.37	+2.03	-5.37	-1.98
Understorey LAI	+14.87	+4.76	-14.87	-4.11
Total ET	+4.13	+3.19	-4.51	-3.04
Total Flow	-10.69	-6.71	+12.21	+7.23

In the case of long-term simulations without interannual climate variability, changing LAI parameters by 10% also led to similar changes in total projected LAI calculated by Macaque (9.7%) (Table 5.3). This was comprised of changes to canopy LAI of +/-6.25% and changes to understorey LAI of +/-13.16%. An increase in total LAI of 9.7% led to an increase in total ET of +4.24%, and a corresponding decrease in total flow of -9.57%. A graphical representation of the effects of changing LAI on long term flow and total ET is provided in Figure 5.1.

Table 5.3. Percentage change of model outputs to changes in LAI for the long term simulation with no interannual climate variability.

	Change in LAI parameters			
	+10%		-10%	
	ΔTotal%	ΔSD%	ΔTotal%	ΔSD%
Total LAI	+9.70	+8.67	-9.70	-8.62
Canopy LAI	+6.25	+1.57	-6.25	-1.52
Understorey LAI	+13.16	+3.73	-13.16	-3.04
Total ET	+4.24	+0.62	-4.71	-0.43
Total Flow	-9.57	-1.43	+10.63	+0.40

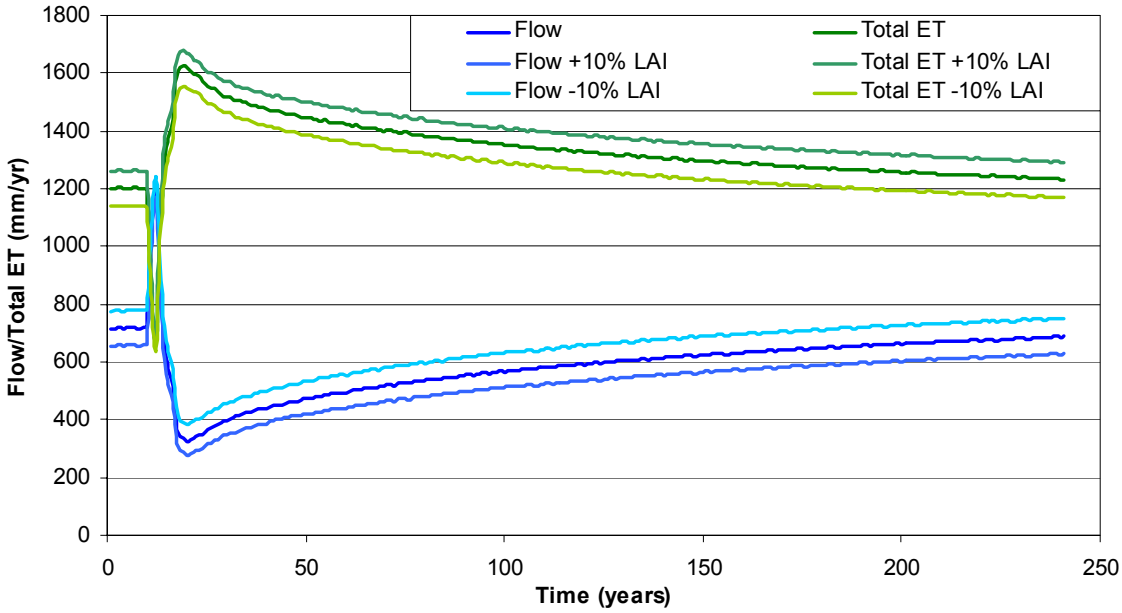

Figure 5.1. Flow and total ET over time with changes in LAI of + and -10%.

5.3 Sensitivity to the conductance with age relationship

To investigate the model sensitivity to changes in conductance, two parameters, representing the maximum canopy leaf conductance and the maximum understorey leaf conductance (see Table 3.2) were together increased and decreased by 10%. Changing these parameters changes the resulting conductance in Macaque by approximately the same proportions. The current default value for these parameters is 0.005. The model was run with both conductance parameters set to 0.0055 (+10%) and then to 0.0045 (-10%) and the resulting outputs of actual conductance, total flow and total ET were examined in a simulation with interannual climate variability and in an simulation with no interannual climate variability.

Changing canopy and understorey maximum conductance parameters by 10% led to similar changes in conductance as calculated by Macaque (9.7-10.2%) for canopy and understorey species. For simulation with interannual climate variability (Table 5.4) changes in conductance of approximately 10% led to changes in total ET of between 2.7 and 3.0%. Corresponding changes in total flow were higher (7.1-7.8%).

Table 5.4. Percentage change of model outputs to changes in conductance for the calibration simulation with interannual variability.

	Change in maximum conductance parameters			
	+10%		-10%	
	ΔTotal%	ΔSD%	ΔTotal%	ΔSD%
Canopy conductance	+9.97	+12.17	-10.07	-11.26
Understorey conductance	+10.13	+11.46	-10.32	-8.99
Total ET	+2.67	+2.85	-2.96	-3.09
Total Flow	-7.08	-3.85	+7.87	+3.96

In long-term simulations, where there is no interannual climate variability, changes in conductance of approximately 10% led to corresponding changes in total ET of between 2.6 and 2.9% (Table 5.5). Corresponding changes in total flow were higher (5.9-6.4%). A graphical representation of the effects of changing conductance on long term flow and total ET is provided in Figure 5.2.

Table 5.5. Percentage change of model outputs to changes in conductance for the long term simulation with no interannual variability.

	Change in maximum conductance parameters			
	+10%		-10%	
	ΔTotal%	ΔSD%	ΔTotal%	ΔSD%
Canopy conductance	+9.72	+8.98	-9.91	-9.25
Understorey conductance	+10.0	+12.7	-10.2	-12.3
Total ET	+2.59	+0.05	-2.85	-0.78
Total Flow	-5.85	-0.49	+6.42	-0.34

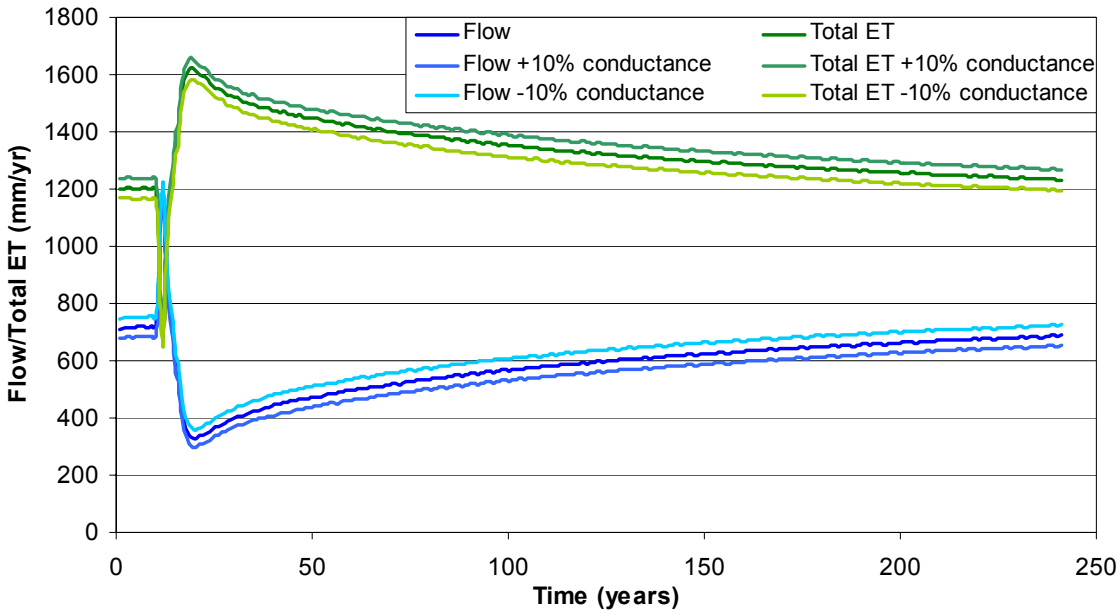

Figure 5.2. Flow and total ET over time with changes in conductance of + and -10%.

5.4 Summary

The relative sensitivities of total flow and total ET to changes in LAI or conductance did not differ greatly between the simulations with variable climate and the long-term simulations with no interannual climate variability. However, flow and ET were slightly more sensitive to change in LAI or conductance with a variable climate.

In relative terms, flow was more sensitive than ET to changes in LAI or conductance. Changes in LAI and conductance affect the amount of water used by vegetation and therefore ET. In percentage terms, changes in ET lead to changes in flow that are twice as large. Flow and ET were both more sensitive to changes in LAI than to changes in conductance. In particular, changes in LAI led to changes in flow of between 9.6 and 12.2%, suggesting that flow is rather sensitive to changes in LAI. This highlights the need to better define values of LAI used in Macaque.

It should be noted that, while changes in relative flow are greater than changes observed in ET, flow is a relatively smaller part of the water balance. In these simulations, flow represents approximately 44% of ET. Therefore, changes in ET produce proportionally larger changes in flow. Therefore, in absolute terms of water volume, a change in ET leads to a lower change in flow from the catchment.

6. Limitations

6.1 Introduction

As with any modelling study, there are limitations to the accuracy of the predictions. These arise from a variety of sources including: data availability, model uncertainty, and processes that are not captured in the modelling framework (including gaps in our understanding of key tree physiological processes across a wide range of species and spatio-temporal scales). Specific limitations of this study are described below.

6.2 Data availability

The spatial and temporal accuracy of the vegetation type and age data in for the catchments contain a degree of uncertainty. In particular, the vegetation age/disturbance history requires a degree of subjective judgment when data are limited or unavailable. For example the age information for mixed species forest is very limited. However, the use of the SFRI vegetation dataset used in this study represents a significant improvement in vegetation type and age data over that used by Peel *et al*. (2000).

Detailed soils information for the catchments were not available for this project, and an assumption was made that the soil is uniform throughout the landscape, despite the fact that we know that this is not the case in the field. The Macaque model is sensitive both to the overall water holding capacity of the soil, and to its transmissivity. These properties vary with soil texture and depth.

Ground truthing of LAI was not possible within the framework of this study. Although NDVI data was obtained, it was not calibrated to the individual catchments. If calibration of NDVI data was possible, then a more accurate assessment of the LAI used in the modelling could be made. Improved representation of LAI in the models would result in an increase in the accuracy of model predictions.

6.3 Model uncertainty

Prediction of water yield is sensitive to subtle variations in the response of plant water use to environmental controls relating to water availability and temperature. These controls were applied within the model primarily through their influence on the conductance of leaf stomata to atmospheric humidity. The parameter values used to model this influence are uncertain, and are based on one or two studies in places like the Pacific northwest of North America, and the Amazon basin; and augmented by calibrations against the expected behaviour of local forests.

It is for this reason that the model sensitivity to changes in the LAI with age and conductance with age relationships was tested. The sensitivity analysis (see Section 5) highlights the importance of good quality LAI measurements and LAI predictions to the water yield results.

Furthermore, the environmental controls on vegetation leaf conductance, those associated with extreme low and high temperatures, are limited in the manner they are represented in Macaque. In Macaque, the temperature inputs are driven by single base station (which is generally not in the catchment), and interpreted across the landscape by the DEM and a simple linear temperature-elevation lapse rate.

6.4 Processes not modelled

Simulations to identify the magnitude and trends of long-term water yield in response to forest change depend largely on the representation of tree transpiration. This present study described tree transpiration in a relatively simple way, by using a set of curves that relate the leaf area index (LAI) of a forest species to the age of that forest species, and then using other curves that relate maximum leaf conductance to age for all eucalypt species. These curves were derived from direct measurements as well as allometric and remote sensing data throughout the Maroondah region in southern Victoria. However, the NDVI data and our understanding of the complexities of natural forests indicate that significant variation in LAI is likely within each species, and between the Maroondah region, and the catchments included in this study. Furthermore, the assumptions of leaf conductance variation with age are largely untested across a range of species. The uncertainty in the ability to represent this relationship accurately has a significant impact on the accuracy of predictions particularly in high water yield impact areas.

The inclusion of a forest growth model in Macaque, where vegetation grows and transpires in response to environmental controls felt to be important, would address this shortcoming, and provide a major improvement to the certainty of model predictions.

7. Vegetation water yield curves

7.1 Introduction

Public native forests in the state of Victoria are managed by the Department of Sustainability and Environment (DSE). They are responsible to ensure that any harvesting of timber from these forests does not adversely impact on water resources.

DSE uses a software program known as the Integrated Forest Planning System (IFPS). This is a linear programming environment that determines the relative benefits of varying forest management strategies. The IFPS is able to evaluate changes in catchment water yield resulting from the harvesting and subsequent regeneration of native forest stands.

The water yield relationship initially embedded in the IFPS was based on an empirical model developed by Kuczera (1987). The so-called 'Kuczera curve' describes how mean annual water yield from a mountain ash (*E. regnans*) forest would vary over the lifecycle of that forest type. The Kuczera curve is based on a statistical analysis of flow records gathered in the Maroondah catchments by Melbourne Water during the period 1910 to 1975. By virtue of the way it is derived, it is a 'regional' curve that gives an average catchment response for forest stands distributed over a wide area with a mean annual rainfall of about 1900mm. The Macaque model (Watson, 1999) was developed specifically to reproduce the Kuczera curve based on spatial and temporal observations of climate and vegetation variables.

In managing the Thomson, Yarra tributaries, Tarago and Bunyip catchments for wood and water supply, DSE needs to know how logging in different parts of these catchments might affect mean annual water yield from the respective catchment. More specific curves are required for each species in each catchment, given the fact that each catchment contains several types of eucalypt stands and other species (not just Mountain Ash) and are each characterised by considerable variation in mean annual rainfall across the catchment.

In an application to the Maroondah and Thomson catchments, Peel *et al*. (2000) demonstrated that Macaque could provide credible estimates of annual water yield across a large and diverse mountainous landscape characterised by a variety of forest species and a broad isohyetal range. A study undertaken later by Peel *et al*. (2002) used Macaque to distill some simple generalisations about the effects of species, stand age and mean annual rainfall on annual water yield. This work led to a set of equations that could be used to estimate annual water yield, requiring only knowledge of the species, stand age and mean annual rainfall. These equations were suitable for direct inclusion into IFPS and resulted in far more credible predictions of forest harvesting impacts on water yield than previous versions of the model that were based on the Kuczera curve.

This section reports on the derivation of a more extensive set of curves, using the methodology described in Peel *et al*. (2002), for different vegetation types in the Thomson, Yarra tributaries, Tarago and Bunyip catchments.

7.2 Extraction and selection of data

In order to estimate the impact of vegetation disturbance on water yield over a long period, a synthetic climate analysis similar to that undertaken by Peel *et al.* (2000) was conducted. An average climate year was first identified for each catchment. The representative year of rainfall was selected to ensure it was close to the average annual rainfall of the base stations for that particular catchment's calibration period, and that the seasonality of that year was similar to the general seasonality of the base stations.

The representative year of rainfall was repeated to create a 300-year rainfall record. The resulting synthetic sequence had no inter-annual variability. The corresponding year records for maximum and minimum temperature were also repeated to create a matching 300-year sequence of maximum and minimum temperatures.

The synthetic sequences were used to run Macaque for 300 years. In this simulation, the age of all vegetation was 250 years at the commencement of the simulation, and was allowed to grow for a further 50 years. Then, all vegetation in the catchment was disturbed and allowed to regrow for a further 250 years.

Macaque generates a temporal sequence and spatial representations of water yield for each year of this synthetic scenario. These temporal sequences describe the impact on water yield of the vegetation regrowth across the catchment.

Ideally, rather than using the average climate methodology of Peel *et al*. (2000) this analysis could be done with stochastically generated precipitation and temperature data that replicate the observed interannual climate variability. However, the number of 300-year model runs required to assess the average water yield impact of vegetation regrowth under stochastic climate replicates, was well beyond the time frame of this project.

Using the synthetic rainfall and temperature sequence, a temporal sequence of annual water yield for every ESU in the catchment was created by Macaque. An example of such a time series is provided in Figure 7.1. The small four-year oscillations observed in this time series represent a small error in handling leap years when creating the synthetic climate. These small oscillations are minor and will not significantly affect the results of any further analysis.

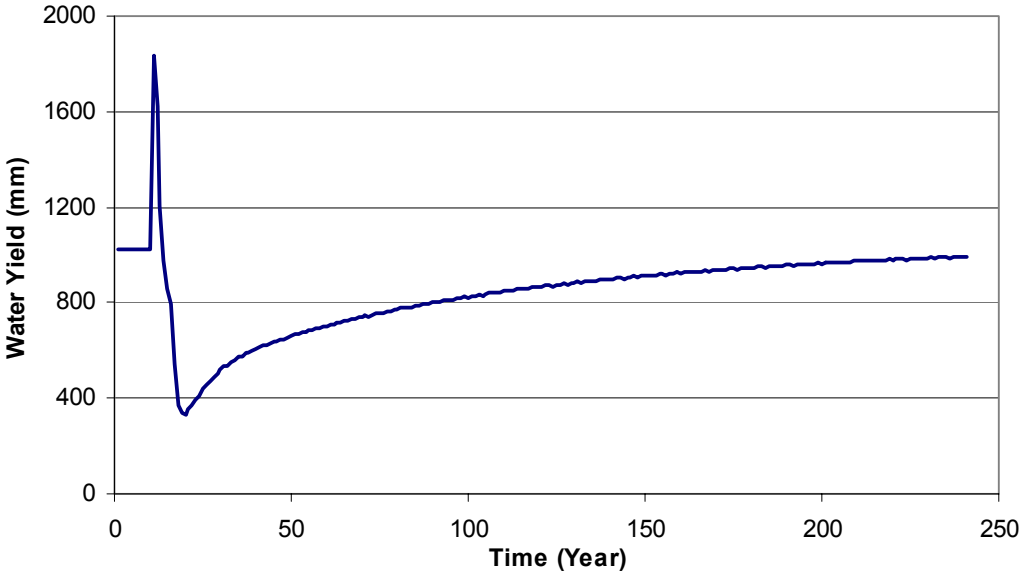

Figure 7.1. An example of an acceptable time series of annual water yield for an ESU representing *E. regnans* in the Thomson catchment.

However, a number of temporal sequences exhibited larger, more random oscillations such as those shown in Figure 7.2. The cause of these oscillations is unknown. These oscillations were also noted by Peel *et al*. (2002) who suggested they were likely to be due to a numerical instability in the Macaque model. Although the oscillations in the water yield curve are large, the average long term shape of the curve remains similar to that observed inFigure 7.1, and therefore catchment-wide conclusions based on the summation of water yield from many ESUs are still likely to be valid. However, the water yield data from ESUs like that shown in Figure 7.2 cannot be used in any further analysis.

The derived curves with oscillations were compared to those without oscillations, to examine whether their exclusion biases the results in anyway. The attributes of these two groups of ESUs (with and without oscillations), including mean annual rainfall, elevation, slope and aspect, were compared for each species. There did not appear to be any differences between the two groups in the four attributes examined (see Appendix A). In addition, the shape of the two groups of curves was compared by visual assessment. The general shape of curves with oscillations did not appear to be noticeably different from the general shape of curves without oscillations. Therefore, removal of these curves from further analysis will not bias the results in any way.

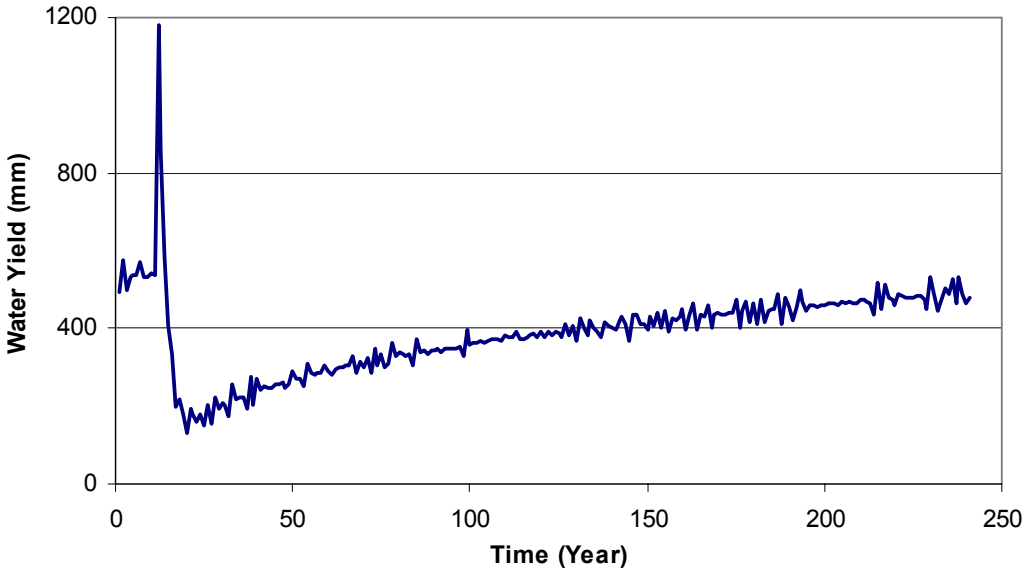

Figure 7.2. An example of an unacceptable time series of annual water yield for an ESU representing mixed spp. in the Thomson catchment due to random oscillations.

A testing tool was developed in which a threshold could be set to identify sequences of water yield that should be considered unacceptable ESUs and could therefore be removed from further analysis. The testing tool was used to analyse all available ESUs, and provided a list of acceptable ESUs where the yield from one year to the next differed by no more than the set threshold. A threshold of about 0.09m was found to be an appropriate threshold for this purpose.

Once the acceptable ESUs have been identified, an Excel macro was used to open the Macaque ESU water yield files and extract the water yield values for each ESU into an Excel spreadsheet for further analysis. Further visual inspection of acceptable ESU time series was conducted. Some ESU time series of water yield were discovered to be zero for several years (over 100 years in some cases) after disturbance, an example of which is shown in Figure 7.3. Even though, it is unlikely that annual water yield should ever equal zero, ESUs where yield was zero for less than 15 years were considered acceptable. Any period longer than 15 years with no flow was considered to be unrealistic and therefore these ESUs were considered unacceptable and not included in further analyses. These yield curves represented ESUs of relatively low rainfall. While there was a bias for these ESUs to be of lower rainfall, the general shape of the yield curves appeared to be the same as those of the remaining ESUs. Inclusion of these derived curves in further analysis would not have altered the resulting model parameters required for the IFPS, because the parameters (as discussed later) primarily influence the amplitude and shape of the curve, and not its absolute water yield.

It was also noted that ESUs where annual water yield was zero for about 20 years or more, generally exhibited a sudden increase in water yield once the yield became positive once more (at 110 years in

Figure 7.3 for example). In addition, these time series of water yield generally proved to poorly fit the water yield curve model.

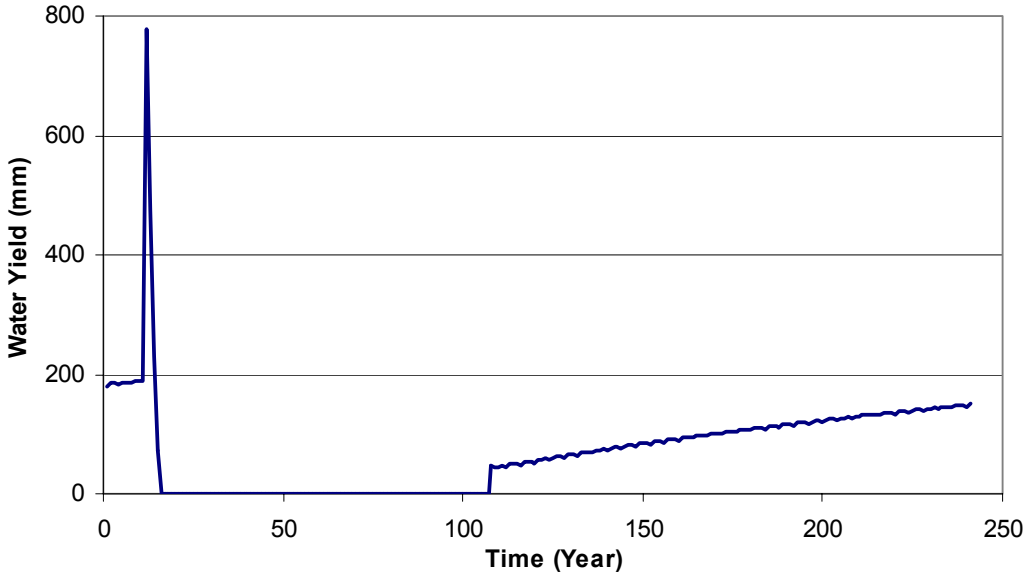

Figure 7.3. An example of an unacceptable time series of annual water yield for an ESU representing mixed spp. in the Thomson catchment due to extended period of zero water yield.

Table 7.1 to Table 7.7 show, for each catchment, the number of ESUs for a particular vegetation type, and the number of those ESUs that were considered acceptable to use for model development. Whether an ESU yield curve was considered acceptable was determined after application of the bulk time series tester tool (see Section 3.3) and visual inspection of time series charts. While the number of acceptable ESUs appears to be low, a reasonable set of model parameters may be obtained from using relatively few curves. The model parameters (see section 8.3) allow the amplitude and shape of the fit to be described. The vertical position of the curve, in terms of its absolute water yield, is defined by the mean annual rainfall of that ESU.

The vegetation classes of water and unknown vegetation were not used in any further analysis. The ESUs considered to be acceptable represent the major vegetation types in the catchments. There were several less abundant vegetation types, represented by only few ESUs, which contained no acceptable ESUs for analysis. No water yield curves can be developed for these vegetation types.

The Excel macro also extracted values of aspect, slope, elevation and mean annual precipitation (MAP) from the Macaque files for each ESU. The values of aspect, slope and elevation were derived from a digital elevation model of each catchment, while the mean annual precipitation values were derived from a multiple linear regression (MLR) analysis of monthly precipitation data and model calibration conducted earlier.

Table 7.1. Number of ESUs with a particular vegetation type, and the number of acceptable ESUs for the Thomson catchment. Percentage of acceptable ESUs is 33.0%.

Vegetation	Code	Number of ESUs	% of all ESUs	Number of acceptable ESUs	% of acceptable ESUs
A. dealbata	25	5	0.34	3	0.80
E. delegatensis	1270	160	11.0	80	21.5
E. nitens	1302	13	0.90	9	2.41
E. pauciflora	1308	8	0.55	7	1.88
E. regnans	1314	208	14.3	57	15.3
E. sieberi	1318	5	0.34	1	0.27
Mixed spp.	9008	713	49.1	205	55.0
Grassland	9011	1	0.1	0	0
Rainforest	9012	3	0.21	3	0.80
Heath	9021	13	0.90	8	2.14
Water	9903	318	21.9	na	na
Not vegetated	9998	4	0.28	na	na
Total		**1451**	**100**	**373**	**100**
Total vegetated		**1129**			

Table 7.2. Number of ESUs with a particular vegetation type, and the number of acceptable ESUs for the Armstrong Creek Main catchment. Percentage of acceptable ESUs is 53.1%.

Vegetation	Code	Number of ESUs	% of all ESUs	Number of acceptable ESUs	% of acceptable ESUs
A. dealbata	25	3	0.97	3	1.83
E. delegatensis	1270	37	12.0	30	18.29
E. nitens	1302	5	1.62	3	1.83
E. regnans	1314	209	67.6	92	56.10
E. sieberi	1318	4	1.29	3	1.83
Mixed spp.	9008	41	13.3	30	18.29
Rainforest	9012	9	2.91	3	1.83
Heath	9021	1	0.32	0	0
Total		**309**	**100**	**164**	**100**

Table 7.3. Number of ESUs with a particular vegetation type, and the number of acceptable ESUs for the Armstrong Creek East catchment. Percentage of acceptable ESUs is 12.2%.

Vegetation	Code	Number of ESUs	% of all ESUs	Number of acceptable ESUs	% of acceptable ESUs
E. regnans	1314	36	29.0	0	0
E. sieberi	1318	3	2.42	2	13.3
Mixed species	9008	84	67.7	13	86.7
Grassland	9011	1	0.81	0	0
Total		**124**	**100**	**15**	**100**

Table 7.4. Number of ESUs with a particular vegetation type, and the number of acceptable ESUs for the McMahons Creek catchment. Percentage of acceptable ESUs is 55.0%.

Vegetation	Code	Number of ESUs	% of all ESUs	Number of acceptable ESUs	% of acceptable ESUs
A. dealbata	25	6	1.51	3	1.37
E. regnans	1314	178	44.7	71	32.4
E. sieberi	1318	15	3.77	15	6.85
Mixed spp.	9008	186	46.7	119	54.3
Rainforest	9012	13	3.27	11	5.02
Total		**398**	**100**	**219**	**100**

Table 7.5. Number of ESUs with a particular vegetation type, and the number of acceptable ESUs for the Starvation Creek catchment. Percentage of acceptable ESUs is 52.3%.

Vegetation	Code	Number of ESUs	% of all ESUs	Number of acceptable ESUs	% of acceptable ESUs
A. dealbata	25	6	1.95	3	1.86
E. delegatensis	1270	1	0.32	1	0.62
E. regnans	1314	154	50.0	70	43.5
E. sieberi	1318	2	0.65	2	1.24
Mixed spp.	9008	121	39.3	68	42.2
Rainforest	9012	16	5.19	10	6.21
Heath	9021	8	2.60	7	4.35
Total		**308**	**100**	**161**	**100**

Table 7.6. Number of ESUs with a particular vegetation type, and the number of acceptable ESUs for the Tarago catchment. Percentage of acceptable ESUs is 89.5%.

Vegetation	Code	Number of ESUs	% of all ESUs	Number of acceptable ESUs	% of acceptable ESUs
A. dealbata	25	24	2.01	23	2.50
E. regnans	1314	466	39.0	412	44.83
E. sieberi	1318	100	8.36	90	9.79
Mixed spp.	9008	255	21.3	227	24.70
Grassland	9011	181	15.1	166	18.06
Rainforest	9012	1	0.08	1	0.11
Water	9903	169	14.1	na	na
Total		**1196**	**100**	**919**	**100**
Total vegetated		**1027**			

Table 7.7. Number of ESUs with a particular vegetation type, and the number of acceptable ESUs for the Bunyip catchment. Percentage of acceptable ESUs is 83.5%.

Vegetation	Code	Number of ESUs	% of all ESUs	Number of acceptable ESUs	% of acceptable ESUs
A. dealbata	25	26	6.48	25	7.46
E. regnans	1314	254	63.34	204	60.90
E. sieberi	1318	7	1.75	7	2.09
Mixed species	9008	106	26.43	94	28.06
Heath	9021	8	2.00	5	1.49
Total		**401**	**100**	**335**	**100**

7.3 Model description

Peel *et al*. (2002) described a simple model for describing the annual water yield at a given ESU for a given vegetation type with the form below in Equation (2).

$$\text{Annual water yield} = \text{MAP} - \text{AET} \quad (2)$$

Where MAP is the mean annual precipitation and AET is the annual actual evapotranspiration at a given ESU. The MAP was extracted from the Macaque output files in the previous section, and therefore AET is the only unknown variable. When using Equation (2) in cases where rainfall is low, it may be possible

that the resulting annual water yield is estimated to be less than zero. In years where a negative water yield is calculated, the annual water yield should be set to equal zero.

Watson *et al*. (1999a) developed a general forest evapotranspiration curve to describe the relationship between forest age and annual evapotranspiration for forests in the Maroondah group of catchments. The form of the Watson *et al*. (1999a) equation is:

$$\begin{aligned} AET = {} & (P1 - P2 - P3) * (e/P5) * AGE * e^{(-AGE/\,P5)} \\ & + (P2 + P3 - P4) * (2/(1+e^{(-AGE/P6)}) - 1) \\ & + P3 * (e^{(-AGE/P7)} - 1) + P4 \end{aligned} \qquad (3)$$

where P1, P2, P3, P4, P5, P6, P7 are parameters and AGE is the age of the forest. Equation (3) is a very flexible relationship and is used in this analysis to describe the relationship between forest age and annual actual evapotranspiration. The flexibility of Equation (3) is sufficient to be able to incorporate the impacts of the relationships between LAI and maximum leaf conductance and forest age on AET.

Parameter values of Equation (3) were determined by fitting the estimate of annual water yield from Equation (2) using AET values from Equation (3) to the Macaque annual water yield curves for acceptable ESUs representing a particular vegetation type. Fitting was done by i) maximising the average E value for predicted yield using the AET from Equation (3) and MAP for each ESU, and ii) using one ESU yield output to assist in fitting the shape of the model by eye. In this way, a single curve for AET over time, represented by Equation (3) (and parameters P1 to P7) is derived for each vegetation type in each catchment. This curve of AET can then be used, with the MAP of a given ESU, to obtain a yield curve using Equation (2).

An example of the Macaque water yield and the modelled water yield derived from Equations (2) and (3) for an ESU representing *E. delegatensis* vegetation in the Thomson catchment is given in Figure 7.4.

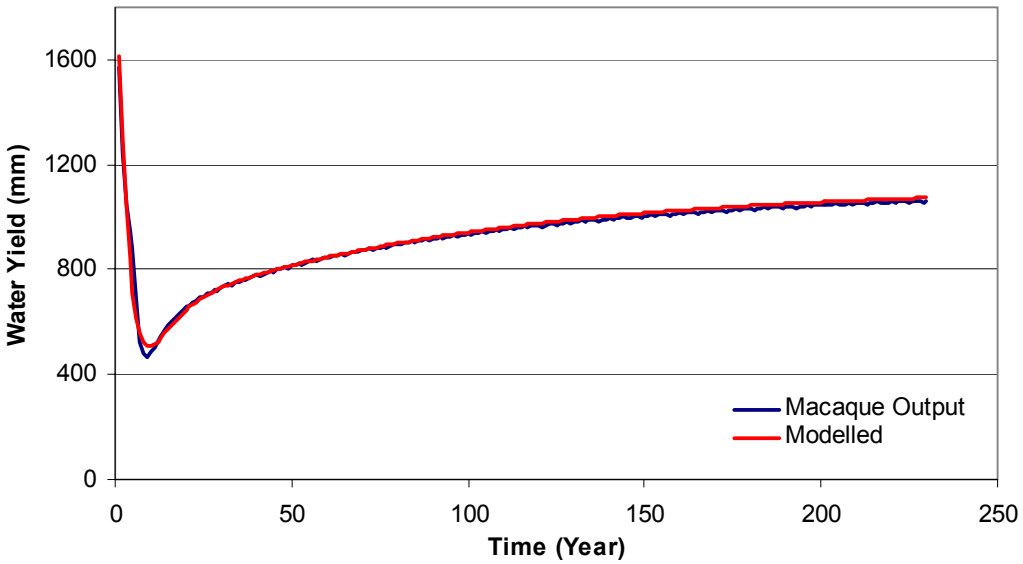

Figure 7.4. Annual water yield from Macaque and model fit for an ESU representing *E. delegatensis* in the Thomson catchment.

The shape of the water yield curve in Figure 7.4 is largely similar to the water yield curves for other ESUs of the same vegetation type. This indicates that the shape of the water yield curve is largely determined by the LAI and maximum leaf conductance relationships with forest age, which are together described by Equation (3). Differences in elevation, aspect and slope between ESUs are largely expected to shift the water yield curve vertically or modify the shape of the water yield curve slightly (Peel *et al*. 2002).

7.4 Model performance

Parameter values of Equation (3) were determined for each vegetation type in each catchment where acceptable ESUs existed. The coefficient of efficiency (E) was again used as an objective measure of model performance, with an E>0.6 considered acceptable. The E value for each water yield record from each acceptable ESU, and that of the model, was determined. The modelling objective was to maximise the average values of E for water yield for each ESU. The resulting distribution of E values also provides a guide to the goodness of the model fit to all ESUs of the respective vegetation type.

If the model was not providing a good fit (as occurred in isolated instances), the inclusion of extra variables into the model, for example elevation, aspect and slope, were considered in order improve the model fit (Peel *et al*. 2002).

7.4.1 Thomson

The distributions of E values for model fit for vegetation types in the Thomson catchment are provided in Table 7.8. The model optimisation produced good results for most vegetation types. A relatively poor model fit was initially achieved for *E. pauciflora*. Peel *et al*. (2002) also observed this, and provided a

revised model that includes a term for slope (Equation 4). This revised model provided a better fit for this data and was also used in this study.

$$\text{Annual water yield} = \text{MAP} - \text{AET} \times (\text{Slope}/11)^{0.1} \quad (4)$$

The model was considered acceptable (where E>0.6) for all ESUs for most vegetation types. The only exception was the model for mixed species, where the model was acceptable for 88% of the ESUs. For many vegetation types, the model fit was extremely good (>0.9) for over 70% of ESUs. The only exception was mixed species, where only 47% of all ESUs showed a very good model fit. It should be remembered that the model fit for *A. dealbata,* rainforest and *E. sieberi* is based on only three or fewer ESUs. The resulting model parameters, P1 to P7, are listed for each vegetation type in Table 7.9.

Table 7.8. Distribution of E values for model fit for vegetation types in the Thomson catchment.

			Distribution of E values for model fit expressed as a percentage of total number of ESUs				
Vegetation	**Total number of ESUs**	**Model acceptability* %**	**<0.6**	**0.6<0.8**	**0.8<0.9**	**0.9<0.95**	**>0.95**
Mixed spp.	205	88	13	18	23	20	27
E. delegatensis	80	100	1	9	23	24	44
E. regnans	57	100	0	12	18	28	42
E. nitens	9	100	0	0	22	33	44
Heath	8	100	0	0	25	0	75
E. pauciflora	7	100	0	14	14	29	43
A. dealbata	3	100	0	0	0	0	100
Rainforest	3	100	0	0	33	33	33
E. sieberi	1	100	0	0	0	0	100

* Percentage of E values above 0.6. The model is considered acceptable when the E value is greater than 0.6.

Table 7.9. Model parameters for vegetation types in the Thomson catchment.

Vegetation	Model form	P1	P2	P3	P4	P5	P6	P7
Mixed spp.	MAP-AET	1540	1120	520	608	35	2	130
E. delegatensis	MAP-AET	1900	1110	520	235	5	2.6	90
E. regnans	MAP-AET	1900	1140	850	150	30	2.2	73
E. nitens	MAP-AET	2130	1630	1040	157	450	2.3	10
Heath	MAP-AET	980	775	245	380	60	2	130
E. pauciflora	MAP-AET x $(Slope/11)^{0.1}$	1150	810	410	550	40	1.9	170
A. dealbata	MAP-AET	1490	1140	430	410	20	2	65
Rainforest	MAP-AET	1330	1030	320	440	20	2.1	65
E. sieberi	MAP-AET	1440	1040	300	470	40	1.5	130

7.4.2 Armstrong Creek Main

The distributions of E values for model fit for vegetation types in the Armstrong Creek Main catchment are provided in Table 7.10. The model performed very well for most vegetation types. The model was considered acceptable (where E>0.6) for all ESUs for most vegetation types. The only exceptions were the models for mixed species and *E. regnans*, where the model was acceptable for 81% and 95% of the ESUs respectively. For many vegetation types, the model fit was extremely good (>0.9) for over 80% of ESUs. The only exceptions were mixed species, rainforest, *E. regnans* and *E. delegatensis,* where 37%, 33% and 62% and 77% of all ESUs showed very good model fits. It should be remembered that the model fit for *E. nitens*, *E. sieberi*, *A. dealbata* and ranforest is based on only three ESUs. The resulting model parameters, P1 to P7, are listed for each vegetation type in Table 7.11.

Table 7.10. Distribution of E values for model fit for the Armstrong Creek Main catchment.

			Distribution of E values for model fit expressed as a percentage of total number of ESUs				
Vegetation	**Total number of ESUs**	**Model acceptability* %**	**<0.6**	**0.6<0.8**	**0.8<0.9**	**0.9<0.95**	**>0.95**
E. regnans	92	95	5	10	23	24	38
E. delegatensis	30	100	0	13	10	17	60
Mixed spp.	30	81	20	27	17	7	30
E. nitens	3	100	0	0	0	0	100
E. sieberi	3	100	0	0	0	33	67
A. dealbata	3	100	0	0	0	0	100
Rainforest	3	100	0	33	33	33	0

* Percentage of E values above 0.6. The model is considered acceptable when the E value is greater than 0.6.

Table 7.11. Model parameters for vegetation types in the Armstrong Creek Main catchment.

Vegetation	Model form	P1	P2	P3	P4	P5	P6	P7
E. regnans	MAP-AET	1816	975	1090	270	45	2.4	138
E. delegatensis	MAP-AET	1958	1096	1130	180	23	2.5	63
Mixed spp.	MAP-AET	1515	985	630	790	57	2.0	270
E. nitens	MAP-AET	1845	1120	625	290	8	2.3	70
E. sieberi	MAP-AET	1324	845	570	690	68	1.8	310
A. dealbata	MAP-AET	1395	1030	430	365	54	1.8	150
Rainforest	MAP-AET	1460	975	350	370	3	2.1	145

7.4.3 Armstrong Creek East

The distributions of E values for model fit for vegetation types in the Armstrong Creek East catchment are provided in Table 7.12. The model performed extremely well for both vegetation types. It should be noted that this is based on two ESUs for each vegetation type. The resulting model parameters, P1 to P7, are listed for each vegetation type in Table 7.13. There were no acceptable ESUs for *E. regnans*, as the output curves fell below zero yield for an extended period, similar to that shown in Figure 8.3. Parameters were estimated by setting the curve minima to the average ratio of yield to rainfall for *E. regnans* from the other catchments and then fitting to the remaining portion (with positive yields) of the ESU output.

Table 7.12. Distribution of E values for model fit for the Armstrong Creek East catchment.

			Distribution of E values for model fit expressed as a percentage of total number of ESUs				
Vegetation	**Total number of ESUs**	**Model acceptability* %**	**<0.6**	**0.6<0.8**	**0.8<0.9**	**0.9<0.95**	**>0.95**
Mixed spp.	13	100	0	15	23	8	54
E. sieberi	2	100	0	0	0	0	100

* Percentage of E values above 0.6. The model is considered acceptable when the E value is greater than 0.6.

Table 7.13. Model parameters for vegetation types in the Armstrong Creek East catchment.

Vegetation	Model form	P1	P2	P3	P4	P5	P6	P7
Mixed spp.	MAP-AET	1535	975	665	720	61	1.9	265
E. sieberi	MAP-AET	1345	840	590	610	80	1.6	320
E. regnans	MAP-AET	1459	420	1065	250	15	1.4	820

7.4.4 McMahons Creek

The distributions of E values for model fit for vegetation types in the McMahons Creek catchment are provided in Table 7.14. The model was considered acceptable (where E>0.6) for all ESUs for most vegetation types. The only exceptions were the models for mixed species and for *E. regnans*, where the model was acceptable for 84% and 98% of ESUs respectively. For many vegetation types, the model fit was extremely good (>0.9) for over 50% of ESUs. It should be noted that the model fit for *A. dealbata* is based on only three ESUs. The resulting model parameters, P1 to P7, are listed for each vegetation type in Table 7.14.

Table 7.14. Distribution of E values for model fit for the McMahons Creek catchment.

			Distribution of E values for model fit expressed as a percentage of total number of ESUs				
Vegetation	**Total number of ESUs**	**Model acceptability* %**	**<0.6**	**0.6<0.8**	**0.8<0.9**	**0.9<0.95**	**>0.95**
Mixed spp.	119	84	15	16	25	19	24
E. regnans	71	98	1	4	13	25	56
E. sieberi	15	100	0	20	27	20	33
Rainforest	11	100	0	36	9	9	45
A. dealbata	3	100	0	33	33	0	33

* Percentage of E values above 0.6. The model is considered acceptable when the E value is greater than 0.6.

Table 7.15. Model parameters for vegetation types in the McMahons Creek catchment.

Vegetation	Model form	P1	P2	P3	P4	P5	P6	P7
E. regnans	MAP-AET	2040	1230	1000	320	25	2.5	70
E. sieberi	MAP-AET	1460	1060	450	790	45	2	190
Mixed spp.	MAP-AET	1580	1060	590	780	50	1.8	270
A. dealbata	MAP-AET	1420	1070	440	490	40	1.8	150
Rainforest	MAP-AET	1390	1010	480	410	40	1.9	140

7.4.5 Starvation Creek

The distributions of E values for model fit for vegetation types in the Starvation Creek catchment are provided in Table 7.16. The model could be optimised very well for most vegetation types. A relatively poor model fit was initially achieved for *E. regnans*. A revised model, including a term for aspect (in degrees), developed for another species type by Peel *et al*. (2002) led to a better model fit. This revised model shown in Equation (5) provided a better fit and was used in this study.

$$\text{Annual water yield} = \text{MAP} - \text{AET} - 11 \times \text{Cos}(0.1 \times \text{Aspect}) \quad (5)$$

The model was considered acceptable (where E>0.6) for all ESUs for most vegetation types. The only exceptions were the models for heath, mixed species and for *E. regnans*, where the model was acceptable for 43%, 90% and 98% of the ESUs respectively. For many vegetation types, the model fit was extremely good (>0.9) for over 70% of ESUs. The only exceptions were *E. sieberi*, heath and mixed species, where only 0%, 14% and 46% of all ESUs showed very good model fits. It should be remembered that the model fit for *A. dealbata*, *E. sieberi* and *E. delegatensis* is based on only three or fewer ESUs. The resulting model parameters, P1 to P7, are listed for each vegetation type in Table 7.17.

Table 7.16. Distribution of E values for model fit for the Starvation Creek catchment.

			Distribution of E values for model fit expressed as a percentage of total number of ESUs				
Vegetation	**Total number of ESUs**	**Model acceptability* %**	**<0.6**	**0.6<0.8**	**0.8<0.9**	**0.9<0.95**	**>0.95**
E. regnans	70	98	3	9	13	24	51
Mixed spp.	68	90	10	22	22	28	18
Rainforest	10	100	0	10	20	40	30
Heath	7	43	57	29	0	0	14
A. dealbata	3	100	0	0	33	0	67
E. sieberi	2	100	0	100	0	0	0
E. delegatensis	1	100	0	0	0	0	100

* Percentage of E values above 0.6. The model is considered acceptable when the E value is greater than 0.6.

Table 7.17. Model parameters for vegetation types in the Starvation Creek catchment.

Vegetation	Model form	P1	P2	P3	P4	P5	P6	P7
E. regnans	MAP – AET – 11 x Cos(0.1 x Aspect)	1820	1036	1030	380	66	2.3	206
E. delegatensis	MAP-AET	2090	1110	1220	100	25	2.1	65
E. sieberi	MAP-AET	1560	1110	530	870	51	2.2	240
Rainforest	MAP-AET	1410	1027	380	360	4	1.7	140
Mixed spp.	MAP-AET	1610	1090	600	870	56	2.3	270
Heath	MAP-AET	965	890	200	270	360	2.3	30
A. dealbata	MAP-AET	1400	1030	420	405	40	1.8	150

7.4.6 Tarago

The distributions of E values for model fit for vegetation types in the Tarago catchment at the dam wall are provided in

Table **7.18**. The model was considered acceptable (where E>0.6) for most ESUs. The poorest model fits were for grassland, *E. sieberi* and *A. dealbata*, where the model was acceptable for 34%, 36% and 65% of ESUs respectively. It should be noted that the model fit for rainforest is based on only one ESU.

A relatively poor model fit was initially achieved for grassland. The ESUs covered by grassland were spread across a wider range of long-term precipitation when compared to all the other vegetation types in the Tarago catchment. More importantly, though, was an even wider range in resulting long-term yields from these ESUs. For other vegetation types, the range of yields tended to be about 30% greater than the range of precipitation they received. For grassland, however, the range in resulting long term yields were greater than 50% of the range in precipitation. It is possible that this resulted from the relatively low evapotranspiration due to the low leaf area index applied to grassland in Macaque. Grassland was modelled with a constant LAI of 1.5, and once disturbed, regained its LAI of 1.5 within 5-10 years (and attained a LAI of 1 after 4 years). If the grassland were not water limited, which occurred during the wetter times of the year, more runoff would have occurred than that in the treed areas of the catchment. Consequently, more frequent and/or more volume of runoff led to an increased range of water yield from ESUs covered by grassland.

It was possible to get the shape of the relationship to replicate the yield curve for most grassland ESUs, however, the overall poor model fit was due to the range of average yield that could not be predicted by the model. There was no relationship between AET and precipitation for grassland as is the case for other species. This results in a large amount of scatter and uncertainty in the predicted versus average water yield plot which could not be removed. Therefore, the application of the model for grassland should be done with extreme caution.

A revised model, including a term for slope (in degrees), developed for another vegetation type by Peel *et al*. (2002) led to a slightly better model fit. This revised model is shown in Equation (6).

$$\text{Annual water yield} = \text{MAP} - \text{AET} \times (\text{Slope} \times 0.17)^{0.16} \quad (6)$$

The resulting model parameters, P1 to P7, are listed for each vegetation type in Table 7.19.

It should be noted that these water yield curves, which were derived for the Tarago catchment as defined by the dam wall (112km^2), are based on calibrated parameters used to calibrate the model of the Tarago subcatchment at Tarago River at Neerim.

During the model calibration phase of this study, it was noted that one of the calibration parameters, the value for the ratio of the hydraulic to surface gradient, tended to increase with increasing catchment size. It is likely, therefore, that this calibration parameter, and possibly the rainfall scaling parameter as well, may change due to catchment size (notwithstanding changes to the observed flow record) if the model had been calibrated to the Tarago Reservoir at the dam wall rather that at Neerim. This in turn would affect the accuracy of the resulting yield curves produced.

Table 7.18. Distribution of E values for model fit for the Tarago catchment.

			Distribution of E values for model fit expressed as a percentage of total number of ESUs				
Vegetation	**Total number of ESUs**	**Model acceptability* %**	**<0.6**	**0.6<0.8**	**0.8<0.9**	**0.9<0.95**	**>0.95**
E. regnans	412	95	6	18	23	32	22
Mixed spp.	227	76	24	21	20	13	22
Grassland	166	34	65	16	11	2	5
E. sieberi	92	36	64	10	8	8	10
A. dealbata	23	65	35	17	9	13	26
Rainforest	1	100	0	0	0	0	100

* Percentage of E values above 0.6. The model is considered acceptable when the E value is greater than 0.6.

Table 7.19. Model parameters for vegetation types in the Tarago catchment.

Vegetation	Model form	P1	P2	P3	P4	P5	P6	P7
E. regnans	MAP-AET	1650	1180	610	250	815	2.3	56
Mixed *spp.*	MAP-AET	1370	790	650	690	46	1.9	300
Grassland	MAP – AET x (Slope x 0.17)$^{0.16}$	820	690	150	460	45	2	100
E. sieberi	MAP-AET	1220	805	465	600	66	1.6	295
A. dealbata	MAP-AET	1203	812	450	330	44	1.6	205
Rainforest	MAP-AET	1100	800	370	190	24	2.1	70

7.4.7 Bunyip

The distributions of E values for model fit for vegetation types in the Bunyip catchment are provided in Table 7.20. The model was considered acceptable (where E>0.6) for all ESUs for only *E. sieberi*. For the other vegetation types of *A. dealbata,* heath, mixed species and *E. regnans* the model was considered acceptable for 72%, 60%, 72% and 94% of the ESUs respectively. For most vegetation types, the model fit was extremely good (>0.9) for over 40% of ESUs. The only exceptions were heath and *A. dealbata*, where 0% and 32% of all ESUs showed very good model fits. The resulting model parameters, P1 to P7, are listed for each vegetation type in Table 7.21.

Table 7.20. Distribution of E values for model fit for the Bunyip catchment.

			Distribution of E values for model fit expressed as a percentage of total number of ESUs				
Vegetation	**Total number of ESUs**	**Model acceptability* %**	**<0.6**	**0.6<0.8**	**0.8<0.9**	**0.9<0.95**	**>0.95**
E. regnans	204	94	6	15	19	35	25
Mixed spp.	94	80	21	20	15	29	16
A. dealbata	25	72	28	28	12	16	16
E. sieberi	7	100	0	14	14	43	29
Heath	5	60	40	0	60	0	0

* Percentage of E values above 0.6. The model is considered acceptable when the E value is greater than 0.6.

Table 7.21. Model parameters for vegetation types in the Bunyip catchment.

Vegetation	Model form	P1	P2	P3	P4	P5	P6	P7
E. regnans	MAP-AET	1710	1025	840	185	63	2.2	185
Mixed spp.	MAP-AET	1510	1012	590	840	46	2.4	265
A. dealbata	MAP-AET	1405	1125	330	625	41	2.0	123
E. sieberi	MAP-AET	1343	858	566	790	62	2.2	395
Heath	MAP-AET	1086	993	157	505	335	1.9	40

7.4.8 Summary

The basic form of the model for describing the annual water yield at a given ESU for a given vegetation type was given in Equation (2). In the process of fitting the model to the Macaque outputs, different values of the parameters (P1 to P7) for estimating the annual evapotranspiration, Equation (3), have been derived for the different vegetation types. In the cases of *E. pauciflora*, *E. obliqua* and mixed species, an extra topographic variable was added to the basic form of the model in order to improve the performance of the model.

The water yield curves representing the vegetation type dependant relationships between annual water yield and stand age were developed from outputs of the Macaque model application to the study catchments. Consequently, the relationships presented here are subject to the assumptions made and limitations of the Macaque model and its application to those catchments, which are discussed in the previous section (Section 6). In particular, the yield predictions for the drier end of the rainfall distribution for each species is likely to be underestimated. Predicted disturbance responses will be a maximum for these parts of the catchments. This is principally due to uncertainties in LAI.

From the results of the model performance, the relationships for describing long-term water yield led to at least satisfactory model performance for most vegetation types across all catchments where they occurred. However, the relationships for vegetation types where the percentage of model acceptability (where E>0.6) is low (e.g. below 60%) and/or the number of acceptable ESUs available for model fitting is low (say, less than 5) should be treated with some caution as they contain a higher level of uncertainty.

The model for *E. pauciflora* in the Thomson catchment includes a slope variable. Values of slope of ESUs with *E. pauciflora* used in the model fitting were between 9.0 and 17.2 degrees. Application of the model for *E. pauciflora* in the Thomson catchment with slope values outside this range should be undertaken with caution.

The model for *E. regnans* in the Starvation Creek catchment includes an aspect variable. Values of aspect of ESUs with *E. regnans* used in the model fitting were between 1 and 355 degrees, covering nearly all

aspects. Therefore, application of the *E. regnans* relationship in the Starvation Creek catchment can be assumed to be appropriate for all values of aspect.

The model for grassland in the Tarago catchment includes a slope variable. Values of slope of ESUs with grassland used in the model fitting were between 0.023 and 18.8 degrees. Application of the model for grassland in the Tarago catchment with aspect values outside this range should be done with extreme caution. In addition, the large amount of scatter and uncertainty in the predicted versus average water yield plots for grassland indicate that the model for grassland should be applied with extreme caution in all circumstances.

The models presented and their respective parameters can only be effectively applied to their catchments as defined by their respective catchment outlets and catchment areas as defined in Table 2.1.

8. Conclusions

The Macaque model was initially developed in the context of research studies into the water balance dynamics of the Maroondah catchment, and has been applied to several other catchments since. While further confidence has been gained in its application to other catchments, the lack of field data and model assumptions limit the ability to validate model results.

Application of Macaque to the catchments of the Thomson, Yarra tributaries (Armstrong Creek Main and East, Cement Creek, Mcahons Creek and Starvation Creek), Tarago and Bunyip catchments resulted in generally good model performance as assessed by the Nash and Suttcliffe E, hydrograph statistics, flow duration curves, and changes in mean, standard deviation and coefficient of variation between modelled and observed streamflow records.

Sensitivity analyses of total flow and total evapotranspiration showed that these outputs were sensitive to changes in LAI and conductance with vegetation age across the whole catchment. Flow was more sensitive than total ET, and both outputs were more sensitive to changes in LAI than to changes in conductance. Changes in LAI of approximately 10% led to changes of between 4.1-4.7% in total ET and in turn led to changes of between 9.6-12.2% in flow. Similar changes in leaf conductance led to changes of between 2.6-2.9% for total ET and between 5.9-7.9% for flow. This highlights the need to conduct field measurements to verify the values of LAI used for a particular catchment.

The calibrated models were then used to derive simple mathematical relationships between forest age and yield for all vegetation classes in every catchment. Adequate model fits were obtained for most ESUs and vegetation types. Some models for selected vegetation types were not acceptable for some of the ESUs and greater uncertainty in their model application should be acknowledged. The exception is the model derived for grassland, which had a very poor acceptability and should be used with extreme caution. Predictions made from these curves probably have a greater level of uncertainty at the drier end of the species-rainfall distribution.

9. References

Beven K.J., Lamb R., Quinn P., Romanowicz R. and Freer J. 1995. TOPMODEL. In: Singh V.P. (ed.) Computer Models of Watershed Hydrology, Water Resources Publications, Highland Ranch, Colorado, 627-668.

Chiew F.H.S., Stewardson M.J. and McMahon T.A. 1993 Comparison of six rainfall-runoff modeling approaches. *Journal of Hydrology,* 147: 1-36.

Cornish P.M. and Vertessy R.A. 2001. Forest age-induced changes in evapotranspiration and water yield in a eucalypt forest. *Journal of Hydrology,* 242: 43-63

Cornish, P.M. 1993. The effects of logging and forest regeneration on water yields in a moist eucalypt forest in New South Wales. *Journal of Hydrology,* 150: 301-322.

Department of Primary Industries and Department of Sustainability and Environment, 2004. Corporate Geospatial Data Library Catalogue. 17th edition. O'Brien, M. (Ed).

Dyer, F. 1998. Sources of sediment and associated phosphorous for Tarago Reservoir. PhD thesis, Department of Civil and Environmental Engineering, The University of Melbourne, Australia.

Efron B. and Tibshirani R.J. 1993. An Introduction to the Bootstrap. Chapman & Hall, New York, 436.

Ellis T.W., Hatton T.J. and Nuberg I.K. 1999. A simple method for estimating recharge from low rainfall agroforestry systems. *In* (Eds A. Musey, L. Santos Pereira and M. Fritsch) Envirowater99, 2nd Inter-Regional Conference on Environment-Water, 1-4 September, Laussane, Switzerland. Presses Polytechnique et Universitaires Romandses, Laussane, 1999.

Kuczera G.A. 1985. Prediction of water yield reductions following a bushfire in ash-mixed species eucalypt forest. Melbourne Metropolitan Board of Works, Melbourne, Vic. Rep. MMBW-W-0014, 163 p.

Kuczera G.A. 1987. Prediction of water yield reductions following a bushfire in ash-mixed species eucalypt forest. *Journal of Hydrology*, 94: 215-236.

Lane P.N.J. and Mackay S.M. 2001. Streamflow response of mixed-species eucalypt forests to patch cutting and thinning treatments. *Forest Ecology and Management,* 143: 131-142.

Langford K.J. 1976. Change in yield of water following a bushfire in a forest of *Eucalyptus regnans*. *Journal of Hydrology* 29: 87-114.

Mein, R.G., Jayasuriya, L.N.N., Jayasuriya, M.D.A. and O'Shaughnessy, P.J. 1993. Simulation of Water Yield to Determine the Impact of Timber Harvesting Strategies for the Thomson Catchment. Proc. Hydro. & Water Res. Symp., Inst. Eng. Aust. Nat. Con. Pub., 93/14. pp 75-80.

Monteith J.L. and Unsworth M.H. 1990. Principles of Environmental Physics (2nd ed.). Routledge, Chapman & Hall, New York, 291pp.

Nash J.E. and Sutcliffe J.V. 1970. River flow forecasting through conceptual models, 1. A discussion of principles. *Journal of Hydrology,* 10: 282-290.

Peel M.C. 1999. Annual runoff variability in a global context. PhD thesis, Dept. of Geography and Environmental Studies, The University of Melbourne, Australia.

Peel M.C., McMahon T.A., Finlayson, B.L. and Watson, F.G.R. 2001. Identification and explanation of continental differences in the variability of annual runoff. *Journal of Hydrology*, 250: 224-240.

Peel M.C., Watson F.G.R., and Vertessy R.A. 2002. Generating water yield curves for forest stands in the Thomson catchment for inclusion in the Intergrated Forest Planning System.

Peel M.C., Watson F.G.R., Vertessy R.A., Lau, J.A., Watson, I.S., Sutton M.W. and Rhodes B.G. 2000. Predicting the water yield impacts of forest disturbance in the Maroondah and Thomson catchments using the Macaque model. Technical Report 00/14, The Cooperative Research Centre for Catchment Hydrology, Melbourne, Australia.

Rawls W.J., Ahuja L.R., Brakensiek D.L. and Shirmohammadi A. 1993. Infiltration and soil water movement,In: Maidment DR (ed.), Handbook of Hydrology, McGraw-Hill, New York, 5.1-5.51.

Roberts, S.L., Vertessy, R.A. and Grayson, R.G. 2001. Transpiration from *Eucalyptus sieberi* (L. Johnson) forests of different age. *Forest Ecology and Management*, 143: 153-161.

Van Genuchten, M.T. 1980. A closed-form equation for predicting the hydraulic conductivity of unsaturated soil. *Soil Scence Society of America Journal*, 44: 892-898.

Vertessy R.A., Hatton T.J., Benyon R.J., Dawes W.R., 1996. Long term growth and water balance predictions for a mountain ash (*Eucalyptus regnans*) forest catchment to clearfelling and regeneration. *Tree Physiology,* 16: 221-232.

Vertessy R.A., Hatton T.J., O'Shaughnessy P.J., Jayasuriya, M.D.A. 1993. Predicting water yield from a mountain ash forest using a terrain analysis-based catchment model. *Journal of Hydrolology*, 150: 665-700.

Vertessy, R.A., Watson, F.G.R. and O'Sullivan, S.K. 2001. Factors determining relations between stand age and catchment water balance in mountain ash forests. *Forest Ecology and Management*, 143: 13-26.

Watson F.G.R., Grayson R.B., Vertessy, R.A. and McMahon T.A. 1998 Large-scale distribution modelling and the utility of detailed ground data. *Hydrological Processes*, 12: 873-888.

Watson F.G.R., Vertessy R.A. and Grayson R.B. 1999a. Large-scale modelling of forest hydrological processes and their long-term effect on water yield. *Hydrological Processes*, 13: 689-700.

Watson F.G.R., Vertessy R.A., McMahon, T.A., Rhodes B.G. and Watson I.S. 1999b. The hydrologic impacts of forestry on the Maroondah catchments. Cooperative research Centre for Catchment Hydrology, Melbourne, Report 99/1, 80pp.

Watson, F.G.R. 1999. Large scale, long term modelling of the effects of land cover change on forest water yield. PhD thesis, Department of Civil and Environmental Engineering, The University of Melbourne, Australia.

Watson, F.G.R., Grayson, R.B., Vertessy, R.A., Peel, M.C. and Pierce, L.L. 2001. Evolution of a Hillslope Hydrologic Model, In MODSIM – International Congress on Modelling and Simulation, Canberra, December, 461-467.

Appendix A. Analysis of acceptable and unacceptable ESUs

Section 7.2 describes the process whereby ESUs were considered acceptable (and used for further analysis) or unacceptable, in which case the water yield with time for a given ESU either contained oscillations, or was negative for more than 20 years. Excluding some ESUs has the potential to lead to a bias when using the remaining ESUs for further analysis. This appendix provides a graphical representation of the characteristics of all ESUs, to highlight any differences between the acceptable and unacceptable ESUs in terms of mean annual rainfall, elevation, aspect and slope. Obvious differences in these characteristics between acceptable and unacceptable ESUs could lead to biases in resulting actual evapotranspiration (AET) functions, where only acceptable ESUs were used.

The analysis was conducted on two different vegetation types (*E. regnans* and mixed species). These were selected as they are two common and abundant vegetation types which are of most interest.

Figure A.1 is a graphical representation of mean annual precipitation, elevation, aspect and slope for each ESU represented by *E. regnans* in the Thomson catchment. The horizontal axis is an arbitrary assignment of a number to each ESU. Of interest, is the relative position of the acceptable and unacceptable ESUs on the vertical axes.

In the case of *E. regnans*, a number of ESUs were excluded on the grounds that the water yield over time was negative for a period longer than 20 years (see pink square symbols in Figure A.1), which was thought to be unreasonable. These ESUs also exhibited a sharp rise in yield, once they became positive, which was uncharacteristic of the expected yield over time. These ESUs represent relatively low mean annual precipitation (MAP) and elevation (Figure A.1 a) and b)).

There appears to be no differences in the aspect and slope of the acceptable and unacceptable ESUs (Figure 1.A.c) and d)).

Figure A.2 is a graphical representation of mean annual precipitation, elevation, aspect and slope for each ESU represented by mixed species in the Thomson catchment. The horizontal axis is an arbitrary assignment of a number to each ESU. Of interest, is the relative position of the acceptable and unacceptable ESUs on the vertical axes.

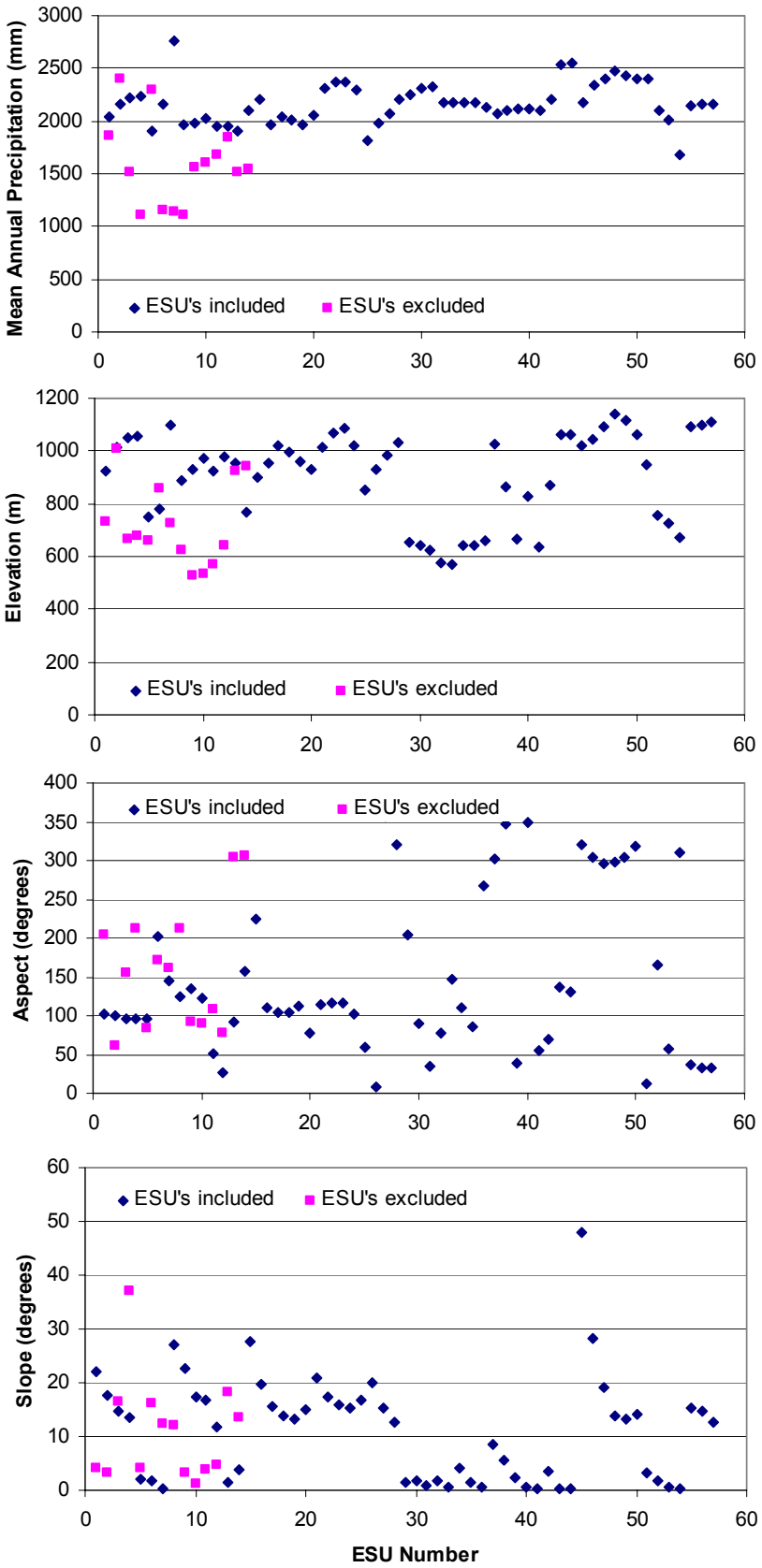

Figure A.1. Plot of a) mean annual rainfall, b) elevation, c) aspect, and d) slope against ESU number for *E. regnans* in the Thomson catchment.

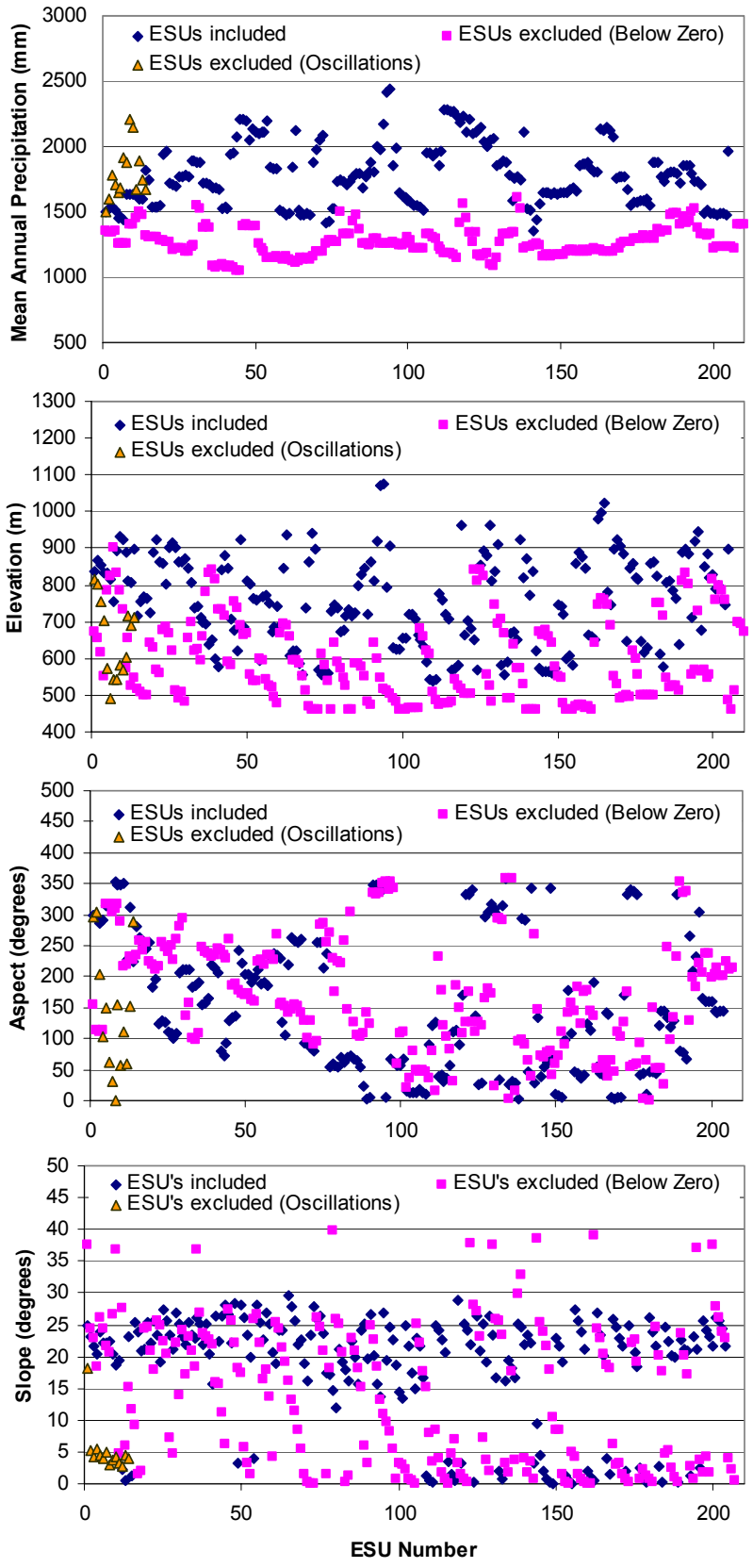

Figure A.2. Plot of a) mean annual rainfall, b) elevation, c) aspect, and d) slope against ESU number for mixed species in the Thomson catchment.

In the case of mixed species, a number of ESUs were excluded on the grounds that the water yield over time was negative (pink squares in Figure A.2), or contained oscillations (orange triangles in Figure A.2). The ESUs with negative water yield over time represent relatively low mean annual precipitation (MAP) and elevation (Figure A.2 a) and b)). There appears to be no differences in the aspect and slope of the acceptable and unacceptable ESUs with negative water yields (Figure 2.A.c) and d)) other than a very small proportion of unacceptable ESUs represented relatively steeper slopes (>30 degrees) than the acceptable ESUs.

The unacceptable ESUs with oscillations (orange triangles in Figure A.2) represent relatively low slopes of between 3 and 5 degrees. The reason for this is unclear. However, this group of ESUs is relatively small, and as it lies within the general population, will not led to a bias in the resulting AET functions.